Available online at www.sciencedirect.com
SCIENCE DIRECT®
Journal of Computational Physics 199 (2004) 663–687
JOURNAL OF COMPUTATIONAL PHYSICS
www.elsevier.com/locate/jcp

An efficient and stable numerical method for the Maxwell–Dirac system

Weizhu Bao *, Xiang-Gui Li

Department of Computational Science, National University of Singapore, Singapore 117543, Singapore

Received 14 January 2004; received in revised form 27 February 2004; accepted 9 March 2004
Available online 12 April 2004

Abstract

In this paper, we present an explicit, unconditionally stable and accurate numerical method for the Maxwell–Dirac system (MD) and use it to study dynamics of MD. As preparatory steps, we take the three-dimensional (3D) Maxwell–Dirac system, scale it to obtain a two-parameter model and review plane wave solution of free MD. Then we present a time-splitting spectral method (TSSP) for MD. The key point in the numerical method is based on a time-splitting discretization of the Dirac system, and to discretize nonlinear wave-type equations by pseudospectral method for spatial derivatives, and then solving the ordinary differential equations (ODEs) in phase space analytically under appropriate chosen transmission conditions between different time intervals. The method is explicit, unconditionally stable, time reversible, time transverse invariant, and of spectral-order accuracy in space and second-order accuracy in time. Moreover, it conserves the particle density exactly in discretized level and gives exact results for plane wave solution of free MD. Extensive numerical tests are presented to confirm the above properties of the numerical method. Furthermore, the tests also suggest the following meshing strategy (or ε-resolution) is admissible in the 'nonrelativistic' limit regime ($0 < \varepsilon \ll 1$): spatial mesh size $h = \mathrm{O}(\varepsilon)$ and time step $\triangle t = \mathrm{O}(\varepsilon^2)$, where the parameter ε is inversely proportional to the speed of light.

Keywords: Maxwell–Dirac system; Time-splitting spectral method; Unconditionally stable; Time reversible; Semiclassical; Plane wave

1. Introduction

One of the fundamental quantum-relativistic equations is given by the Maxwell–Dirac system (MD), i.e. the Dirac equation [16,28] for the electron as a spinor coupled to the Maxwell equations for the electromagnetic field. It represents the time-evolution of fast (relativistic) electrons and positrons within self-consistent generated electromagnetic fields. In its most compact form, the Dirac equation reads [8,17,23,27]

* Corresponding author. Tel.: +65-6874-3337; fax: +65-6774-6756.
E-mail addresses: bao@cz3.nus.edu.sg (W. Bao), xianggui-li@vip.sina.com (X.-G. Li).
URL: http://www.cz3.nus.edu.sg/~bao/.

0021-9991/$ - see front matter
doi:10.1016/j.jcp.2004.03.003

$$\left(\mathrm{i}\hbar\gamma^{\eta}\partial_{\eta} - m_0 c + e\gamma^{\eta}A_{\eta}\right)\Psi = 0. \tag{1.1}$$

Here the unknown Ψ is the 4-vector complex wave function of the "spinorfield": $\Psi(t,\mathbf{x}) = (\Psi_1,\Psi_2,\Psi_3,\Psi_4)^{\mathrm{T}} \in \mathbb{C}^4$, $x_0 = ct$, $\mathbf{x} = (x_1,x_2,x_3)^{\mathrm{T}} \in \mathbb{R}^3$ with $x_0, \mathbf{x}$ denoting the time – resp. spatial coordinates in Minkowski space. ∂_{η} stands for $\frac{\partial}{\partial x_{\eta}}$, i.e. $\partial_0 = \frac{\partial}{\partial x_0} = \frac{1}{c}\frac{\partial}{\partial t}$, $\partial_k = \frac{\partial}{\partial x_k}$ $(k = 1,2,3)$, where we consequently adopt notation that Greek letter η denotes 0, 1, 2, 3 and k denotes the three spatial dimension indices 1, 2, 3. $\gamma^{\eta}A_{\eta}$ stands for the summation $\sum_{\eta=0}^{3}\gamma^{\eta}A_{\eta}$. The physical constants are: $\hbar$ for the Planck constant, c for the speed of light, m_0 for the electron's rest mass, and e for the unit charge. By $\gamma^{\eta} \in \mathbb{C}^{4\times 4}$, $\eta = 0,\ldots,3$, we denote the 4×4 Dirac matrices given by

$$\gamma^0 = \begin{pmatrix} \mathbb{I}_2 & 0 \\ 0 & -\mathbb{I}_2 \end{pmatrix}, \quad \gamma^k = \begin{pmatrix} 0 & \sigma^k \\ -\sigma^k & 0 \end{pmatrix}, \quad k = 1,2,3,$$

where $\mathbb{I}_m$ (m a positive integer) is the $m\times m$ identity matrix and σ^k $(k = 1,2,3)$ the 2×2 Pauli matrices, i.e.

$$\sigma^1 := \begin{pmatrix} 0 & 1 \\ 1 & 0 \end{pmatrix}, \quad \sigma^2 := \begin{pmatrix} 0 & -\mathrm{i} \\ \mathrm{i} & 0 \end{pmatrix}, \quad \sigma^3 := \begin{pmatrix} 1 & 0 \\ 0 & -1 \end{pmatrix}.$$

$A_{\eta}(t,\mathbf{x}) \in \mathbb{R}$, $\eta = 0,\ldots,3$, are the components of the time-dependent electromagnetic potential, in particular $V(t,\mathbf{x}) = -A_0(t,\mathbf{x})$ is the electric potential and $\mathbf{A}(t,\mathbf{x}) = (A_1,A_2,A_3)^{\mathrm{T}}$ is the magnetic potential vector. Hence the electric and magnetic fields are given by

$$\mathbf{E}(t,\mathbf{x}) = \nabla A_0 - \partial_t\mathbf{A} = -\nabla V - \partial_t\mathbf{A}, \quad \mathbf{B}(t,\mathbf{x}) = \operatorname{curl}\mathbf{A} = \nabla\times\mathbf{A}. \tag{1.2}$$

In order to determine the electric and magnetic potentials from fields uniquely, we have to choose a gauge. In practice, the Lorentz gauge condition is often introduced

$$L(t,\mathbf{x}) := \frac{1}{c}\partial_t V + \nabla\cdot\mathbf{A} = -\frac{1}{c}\partial_t A_0 + \nabla\cdot\mathbf{A} = 0. \tag{1.3}$$

Thus the electric and magnetic fields are governed by the Maxwell equation:

$$-\frac{1}{c}\partial_t\mathbf{E} + \nabla\times\mathbf{B} = \frac{1}{c\epsilon_0}\mathbf{J}, \quad \nabla\cdot\mathbf{B} = 0, \tag{1.4}$$

$$\frac{1}{c}\partial_t\mathbf{B} + \nabla\times\mathbf{E} = \mathbf{0}, \quad \nabla\cdot\mathbf{E} = \frac{1}{\epsilon_0}\rho, \tag{1.5}$$

where ϵ_0 is the permittivity of the free space. The particle density ρ and current density $\mathbf{J} = (j_1,j_2,j_3)^{\mathrm{T}}$ are defined as follows:

$$\rho = e|\Psi|^2 := e\sum_{j=1}^{4}|\Psi_j|^2, \quad j_k = ec\langle\Psi,\alpha^k\Psi\rangle := ec\bar{\Psi}^{\mathrm{T}}\alpha^k\Psi, \quad k = 1,2,3, \tag{1.6}$$

where $\bar{f}$ denotes the conjugate of f and

$$\alpha^k = \gamma^0\gamma^k = \begin{pmatrix} 0 & \sigma^k \\ \sigma^k & 0 \end{pmatrix}, \quad k = 1,2,3. \tag{1.7}$$

From now on, we adopt the standard notations $|\cdot|$, $\langle\cdot,\cdot\rangle$ and $\|\cdot\|$ for l^2-norm of a vector, inner product and L^2-norm of a function.

Separating the time derivative associated to the "relativistic time variable" $x_0 = ct$ and applying γ^0 from left of (1.1), plugging (1.2) into (1.4) and (1.5), noticing (1.3), we have the following Maxwell–Dirac system [26]

$$\mathrm{i}\hbar\partial_t \Psi = \sum_{k=1}^{3} \alpha^k (-\mathrm{i}\hbar c\partial_k - eA_k)\Psi + eV\Psi + m_0 c^2 \beta \Psi, \tag{1.8}$$

$$\left(\frac{1}{c^2}\partial_t^2 - \Delta\right) V = \frac{1}{\epsilon_0}\rho, \quad \left(\frac{1}{c^2}\partial_t^2 - \Delta\right)\mathbf{A} = \frac{1}{c\epsilon_0}\mathbf{J}. \tag{1.9}$$

The vector wave function Ψ is normalized as

$$\|\Psi(t,\cdot)\|^2 := \int_{\mathbb{R}^3} |\Psi(t,\mathbf{x})|^2 \, \mathrm{d}\mathbf{x} = 1. \tag{1.10}$$

The MD system (1.8) and (1.9) represents the time-evolution of fast (relativistic) electrons and positrons within self-consistent generated electromagnetic fields. From the mathematical point of view, the strongly nonlinear MD system poses a hard problem in the study of PDEs arising from quantum physics. Well posedness and existence of solutions on all of $\mathbb{R}^3$ but only locally in time has been proved almost 40 years ago [11,12,21]. In particular, there are no global existence results without smallness assumptions on the initial data [19,20]. Thus the MD system is quite involved from the numerical point of view as it poses major open problems from analytical point of view. For solitary solution of MD, we refer [1,10,13,14,23].

The aim of this paper is to design an explicit, unconditionally stable and accurate numerical method for the MD system and apply it to study dynamics of MD. The key point in the numerical method is based on a time-splitting discretization of the Dirac system (1.8), which was used successfully to solve nonlinear Schrödinger equation (NLS) [2–5] and Zakharov system [6,7], and to discretize the nonlinear wave-type equation (1.9) by pseudospectral method for spatial derivatives, and then solving the ODEs in phase space analytically under appropriate chosen transmission conditions between different time intervals.

The paper is organized as follows. In Section 2, we start out with the MD, scale it to get a two-parameter model and review plane wave solution of free MD. In Section 3, we present a time-splitting spectral method (TSSP) for the MD and show some properties of the numerical method. In Section 4, numerical tests of MD for different cases are reported to demonstrate efficiency and high resolution of our numerical method. In Section 5 a summary is given.

2. The Maxwell–Dirac system

Consider the Maxwell–Dirac system represents the time-evolution of fast (relativistic) electrons and positrons within external and self-consistent generated electromagnetic fields [26]

$$\mathrm{i}\hbar\partial_t \Psi = \sum_{k=1}^{3} \alpha^k \left[-\mathrm{i}\hbar c\partial_k - e\left(A_k + A_k^{\mathrm{ext}}\right)\right]\Psi + e(V + V^{\mathrm{ext}})\Psi + m_0 c^2 \beta \Psi, \tag{2.1}$$

$$\left(\frac{1}{c^2}\partial_t^2 - \Delta\right) V = \frac{1}{\epsilon_0}\rho, \quad \left(\frac{1}{c^2}\partial_t^2 - \Delta\right)\mathbf{A} = \frac{1}{c\epsilon_0}\mathbf{J}, \tag{2.2}$$

where $V^{\rm ext} = V^{\rm ext}(t,\mathbf{x}) \in \mathbb{R}$ and $\mathbf{A}^{\rm ext}(t,\mathbf{x}) = (A_1^{\rm ext}, A_2^{\rm ext}, A_3^{\rm ext})^{\rm T} \in \mathbb{R}^3$ are the external electric and magnetic potentials, respectively.

2.1. Dimensionless Maxwell–Dirac system

We rescale the MD (2.1) and (2.2) under the normalization (1.10) by introducing a reference velocity v, length $L = e^2/m_0v^2\epsilon_0$, time $T = v/L$, and strength of the electromagnetic potential $\lambda = e/L\epsilon_0$, as

$$\tilde{\mathbf{x}} = \frac{\mathbf{x}}{L}, \quad \tilde{t} = \frac{t}{T}, \quad \tilde{\Psi}(\tilde{t},\tilde{\mathbf{x}}) = L^{3/2}\Psi(t,\mathbf{x}), \quad \tilde{V}(\tilde{t},\tilde{\mathbf{x}}) = \lambda V(t,\mathbf{x}), \tag{2.3}$$

$$\tilde{\mathbf{A}}(\tilde{t},\tilde{\mathbf{x}}) = \lambda\mathbf{A}(t,\mathbf{x}), \quad \tilde{\mathbf{A}}^{\rm ext}(\tilde{t},\tilde{\mathbf{x}}) = \lambda\mathbf{A}^{\rm ext}(t,\mathbf{x}), \quad \tilde{V}^{\rm ext}(\tilde{t},\tilde{\mathbf{x}}) = \lambda V^{\rm ext}(t,\mathbf{x}). \tag{2.4}$$

Plugging (2.3) and (2.4) into (2.1) and (2.2), then removing all $\tilde{}$, we get the following dimensionless MD:

$$\mathrm{i}\delta\partial_t\Psi = -\mathrm{i}\frac{\delta}{\varepsilon}\sum_{k=1}^{3}\alpha^k\partial_k\Psi - \sum_{k=1}^{3}\alpha^k(A_k + A_k^{\rm ext})\Psi + (V + V^{\rm ext})\Psi + \frac{1}{\varepsilon^2}\beta\Psi, \tag{2.5}$$

$$\big(\varepsilon^2\partial_t^2 - \Delta\big)V = \rho, \quad \big(\varepsilon^2\partial_t^2 - \Delta\big)\mathbf{A} = \varepsilon\mathbf{J}. \tag{2.6}$$

Two important dimensionless parameters in the MD (2.5) and (2.6) are given by the ratio of the reference velocity to the speed of light, i.e. ε, and the scaled Planck constant, i.e. δ, as

$$\varepsilon := \frac{v}{c}, \quad \delta := \frac{\hbar\epsilon_0 v}{e^2}. \tag{2.7}$$

The position and current densities, Lorentz gauge, as well as electric and magnetic fields in dimensionless variables are

$$\rho(t,\mathbf{x}) = |\Psi(t,\mathbf{x})|^2, \quad j_k(t,\mathbf{x}) = \frac{1}{\varepsilon}\langle\Psi(t,\mathbf{x}),\alpha^k\Psi(t,\mathbf{x})\rangle, \quad k = 1,2,3, \tag{2.8}$$

$$L(t,\mathbf{x}) = \varepsilon\partial_t V(t,\mathbf{x}) + \nabla\cdot\mathbf{A}(t,\mathbf{x}), \quad t \geqslant 0, \ \ \mathbf{x}\in\mathbb{R}^3, \tag{2.9}$$

$$\mathbf{E}(t,\mathbf{x}) = -\varepsilon\partial_t\mathbf{A}(t,\mathbf{x}) - \nabla V(t,\mathbf{x}), \quad \mathbf{B}(t,\mathbf{x}) = \nabla\times\mathbf{A}(t,\mathbf{x}). \tag{2.10}$$

When $v \approx c$ and choosing $v = c$, then $\varepsilon = 1$ in (2.7) and the MD (2.5) and (2.6) collapse to a one-parameter model which is used in [26] to study classical limit and semiclassical asymptotics of MD. In this case, the parameter δ is the same as the canonical parameter α used in physical literatures [16,28]. When $v \ll c$ and choosing $v = e^2/\hbar\epsilon_0$, then $\delta = 1$ and $0 < \varepsilon \ll 1$ in (2.7), again the MD (2.5) and (2.6) collapse to a one-parameter model which is called as 'nonrelativistic' limit regime and used in [8,9,18,22,24,25] to study semi-nonrelativistic limits of MD, i.e. letting $\varepsilon \to 0$ in (2.5) and (2.6). For electrons, $\varepsilon = 1$ and $\delta \approx 10.9149$ [26].

The MD system (2.5) and (2.6) together with initial data

$$\Psi(0,\mathbf{x}) = \Psi^{(0)}(\mathbf{x}) \quad \text{with } \|\Psi^{(0)}\| = \int_{\mathbb{R}^3}|\Psi^{(0)}(\mathbf{x})|^2\,\mathrm{d}\mathbf{x} = 1, \tag{2.11}$$

$$V(0,\mathbf{x}) = V^{(0)}(\mathbf{x}), \quad \partial_t V(0,\mathbf{x}) = V^{(1)}(\mathbf{x}), \quad \mathbf{x}\in\mathbb{R}^3, \tag{2.12}$$

$$\mathbf{A}(0,\mathbf{x}) = \mathbf{A}^{(0)}(\mathbf{x}), \quad \partial_t\mathbf{A}(0,\mathbf{x}) = \mathbf{A}^{(1)}(\mathbf{x}) \tag{2.13}$$

is time-reversible and time-transverse invariant, i.e., if constants α_0 and α_1 are added to $V^{(0)}$ and $V^{(1)}$, respectively, in (2.12), then the solution V get added by $\alpha_0 + \alpha_1 t$ and Ψ get multiplied by $e^{-it(\alpha_0+\alpha_1 t/2)/\delta}$, which leaves density of each particle $|\psi_j|$ $(j = 1, 2, 3, 4)$ unchanged. Moreover, multiplying (2.5) by $\bar{\Psi}$ and taking imaginary parts we obtain the conservation law

$$\partial_t \rho(t, \mathbf{x}) + \nabla \cdot \mathbf{J}(t, \mathbf{x}) = 0, \quad t \geqslant 0, \ \ \mathbf{x} \in \mathbb{R}^3. \tag{2.14}$$

From (2.14) and (2.6), we get the Lorentz gauge of the MD system (2.5) and (2.6) satisfying

$$\left(\varepsilon^2 \partial_t^2 - \Delta\right) L(t, \mathbf{x}) = \varepsilon(\partial_t \rho + \nabla \cdot \mathbf{J}) = 0, \quad t \geqslant 0, \ \ \mathbf{x} \in \mathbb{R}^3, \tag{2.15}$$

$$L(0, \mathbf{x}) = \varepsilon \partial_t V(0, \mathbf{x}) + \nabla \cdot \mathbf{A}(0, \mathbf{x}) = \varepsilon V^{(1)}(\mathbf{x}) + \nabla \cdot \mathbf{A}^{(0)}(\mathbf{x}), \tag{2.16}$$

$$\begin{aligned} \partial_t L(0, \mathbf{x}) &= \varepsilon \partial_{tt} V(0, \mathbf{x}) + \nabla \cdot \partial_t \mathbf{A}(0, \mathbf{x}) = \frac{1}{\varepsilon}[\rho(0, \mathbf{x}) + \Delta V(0, \mathbf{x})] + \nabla \cdot \mathbf{A}^{(1)}(\mathbf{x}) \\ &= \frac{1}{\varepsilon}\left[\Delta V^{(0)}(\mathbf{x}) + |\Psi^{(0)}(\mathbf{x})|^2 + \varepsilon \nabla \cdot \mathbf{A}^{(1)}(\mathbf{x})\right], \quad \mathbf{x} \in \mathbb{R}^3. \end{aligned} \tag{2.17}$$

Thus if the initial data in (2.11)–(2.13) satisfy

$$\varepsilon V^{(1)}(\mathbf{x}) + \nabla \cdot \mathbf{A}^{(0)}(\mathbf{x}) \equiv 0, \quad \Delta V^{(0)}(\mathbf{x}) + |\Psi^{(0)}(\mathbf{x})|^2 + \varepsilon \nabla \cdot \mathbf{A}^{(1)}(\mathbf{x}) \equiv 0, \quad \mathbf{x} \in \mathbb{R}^3, \tag{2.18}$$

which implies

$$L(0, \mathbf{x}) = 0, \quad \partial_t L(0, \mathbf{x}) = 0, \quad \mathbf{x} \in \mathbb{R}^3, \tag{2.19}$$

the gauge is henceforth conserved during the time-evolution of the MD (2.5) and (2.6).

2.2. Plane wave solution

If the initial data in (2.11)–(2.13) for the MD (2.5) and (2.6) are chosen as

$$\Psi^{(0)}(\mathbf{x}) = \Psi^{(0)} e^{i\omega \cdot \mathbf{x}} = \Psi^{(0)} e^{i(\omega_1 x_1 + \omega_2 x_2 + \omega_3 x_3)}, \tag{2.20}$$

$$V^{(0)}(\mathbf{x}) \equiv V^{(0)}, \quad V^{(1)}(\mathbf{x}) \equiv V^{(1)}, \quad \mathbf{x} \in \mathbb{R}^3, \tag{2.21}$$

$$\mathbf{A}^{(0)}(\mathbf{x}) \equiv \mathbf{A}^{(0)} = \begin{pmatrix} A_1^{(0)} \\ A_2^{(0)} \\ A_3^{(0)} \end{pmatrix}, \quad \mathbf{A}^{(1)}(\mathbf{x}) \equiv \mathbf{A}^{(1)} = \begin{pmatrix} A_1^{(1)} \\ A_2^{(1)} \\ A_3^{(1)} \end{pmatrix}, \tag{2.22}$$

where $\omega = (\omega_1, \omega_2, \omega_3)^{\mathrm{T}}$ with ω_j $(j = 1, 2, 3)$ integers, $V^{(0)}$, $V^{(1)}$ constants, $\Psi^{(0)}$, $\mathbf{A}^{(0)}$, $\mathbf{A}^{(1)}$ constant vectors, and

$$\Psi^{(0)} = \frac{1}{4\pi\sqrt{\pi}\sqrt{\delta^{-2} + |\omega|^2 - \delta^{-1}\sqrt{\delta^{-2} + |\omega|^2}}} \begin{pmatrix} \omega_3 \\ \omega_1 + i\omega_2 \\ \sqrt{\delta^{-2} + |\omega|^2} - \delta^{-1} \\ 0 \end{pmatrix},$$

then the MD (2.5) and (2.6) with $\varepsilon = 1$, $\mathbf{A}^{\text{ext}} = -\mathbf{A}$ and $V^{\text{ext}} = -V$, i.e. free MD [15], admits the following plane wave solution:

$$\Psi(t,\mathbf{x}) = \Psi^{(0)} \exp\left(\mathrm{i}\omega\cdot\mathbf{x} - \mathrm{i}t\sqrt{\delta^{-2} + |\omega|^2}\right), \tag{2.23}$$

$$V(t,\mathbf{x}) = -V^{\text{ext}} = V^{(0)} + V^{(1)}t + \frac{1}{16\pi^3}t^2, \quad \mathbf{x}\in\mathbb{R}^3, \ \ t \geqslant 0, \tag{2.24}$$

$$\mathbf{A}(t,\mathbf{x}) = -\mathbf{A}^{\text{ext}} = \mathbf{A}^{(0)} + \mathbf{A}^{(1)}t + \frac{1}{2}\mathbf{J}^{(0)}t^2, \tag{2.25}$$

where $\mathbf{J}^{(0)} = (j_1^{(0)}, j_2^{(0)}, j_3^{(0)})^{\mathrm{T}}$ and

$$j_k^{(0)} = \frac{\omega_k}{8\pi^3\sqrt{\delta^{-2} + |\omega|^2}}, \quad k = 1,2,3.$$

Here the normalization condition for the wave function is set as

$$\int_{-\pi}^{\pi}\int_{-\pi}^{\pi}\int_{-\pi}^{\pi} |\Psi(t,\mathbf{x})|^2 \,\mathrm{d}\mathbf{x} = 1.$$

3. Numerical method

In this section we present an explicit, unconditionally stable and accurate numerical method for the MD (2.5) and (2.6). We shall introduce the method in 3D on a box with periodic boundary conditions. For 3D in a box $\Omega = [a_1,b_1]\times[a_2,b_2]\times[a_3,b_3]$, the problem with initial and boundary conditions become

$$\mathrm{i}\delta\partial_t\Psi = -\mathrm{i}\frac{\delta}{\varepsilon}\sum_{k=1}^{3}\alpha^k\partial_k\Psi - \sum_{k=1}^{3}\alpha^k(A_k + A_k^{\text{ext}})\Psi + (V + V^{\text{ext}})\Psi + \frac{1}{\varepsilon^2}\beta\Psi, \tag{3.1}$$

$$\left(\varepsilon^2\partial_t^2 - \Delta\right)V(t,\mathbf{x}) = \rho, \quad \left(\varepsilon^2\partial_t^2 - \Delta\right)\mathbf{A}(t,\mathbf{x}) = \varepsilon\mathbf{J}, \quad \mathbf{x}\in\Omega, \quad t > 0, \tag{3.2}$$

$$\Psi(0,\mathbf{x}) = \Psi^{(0)}(\mathbf{x}), \quad V(0,\mathbf{x}) = V^{(0)}(\mathbf{x}), \quad \partial_t V(0,\mathbf{x}) = V^{(1)}(\mathbf{x}), \tag{3.3}$$

$$\mathbf{A}(0,\mathbf{x}) = \mathbf{A}^{(0)}(\mathbf{x}), \quad \partial_t\mathbf{A}(0,\mathbf{x}) = \mathbf{A}^{(1)}(\mathbf{x}), \quad \mathbf{x}\in\Omega \tag{3.4}$$

$$\text{with periodic boundary conditions for } \Psi, V, \mathbf{A} \text{ on } \partial\Omega, \tag{3.5}$$

where $V^{(1)}$ and $\mathbf{A}^{(0)}$ satisfy

$$\varepsilon V^{(1)}(\mathbf{x}) + \nabla\cdot\mathbf{A}^{(0)}(\mathbf{x}) = 0, \quad \mathbf{x}\in\Omega \tag{3.6}$$

and the normalization condition for the wave function is set as

$$\|\Psi(t,\cdot)\|^2 := \int_\Omega |\Psi(t,\mathbf{x})|^2\,\mathrm{d}\mathbf{x} = \int_\Omega |\Psi^{(0)}(\mathbf{x})|^2\,\mathrm{d}\mathbf{x} = 1. \tag{3.7}$$

Moreover, integrating the first equation in (3.2) we obtain

$$\varepsilon^2 \frac{\mathrm{d}^2}{\mathrm{d}t^2} \int_\Omega V(t,\mathbf{x})\,\mathrm{d}\mathbf{x} = \int_\Omega \rho(t,\mathbf{x})\,\mathrm{d}\mathbf{x} = \int_\Omega |\Psi(t,\mathbf{x})|^2\,\mathrm{d}\mathbf{x} = 1, \quad t \geqslant 0. \tag{3.8}$$

This implies that

$$\mathrm{Mean}(V(t,\cdot)) = \mathrm{Mean}(V^{(0)}) + t\,\mathrm{Mean}(V^{(1)}) + \frac{t^2}{2\varepsilon^2}, \quad t \geqslant 0, \tag{3.9}$$

where

$$\mathrm{Mean}(f) := \int_\Omega f(\mathbf{x})\,\mathrm{d}\mathbf{x}.$$

3.1. Time-splitting spectral discretization

We choose the spatial mesh size $h_j = \frac{b_j - a_j}{M_j}$ $(j = 1,2,3)$ in x_j-direction with M_j given integer and time step Δt. Denote the grid points as

$$\mathbf{x}_{p,q,r} = (x_{1,p}, x_{2,q}, x_{3,r})^{\mathrm{T}} \quad (p,q,r) \in \mathcal{N},$$

where

$$\mathcal{N} = \{(p,q,r) \mid 0 \leqslant p \leqslant M_1,\ 0 \leqslant q \leqslant M_2,\ 0 \leqslant r \leqslant M_3\},$$
$$x_{1,p} = a_1 + ph_1, \quad x_{2,q} = a_2 + qh_2, \quad x_{3,r} = a_3 + rh_3 \quad (p,q,r) \in \mathcal{N}$$

and time step as

$$t_n = n\Delta t, \quad t_{n+1/2} = (n+1/2)\Delta t, \quad n = 0,1,\ldots$$

Let $\Psi^n_{p,q,r}$, $V^n_{p,q,r}$ and $\mathbf{A}^n_{p,q,r}$ be the numerical approximation of $\Psi(t_n,\mathbf{x}_{p,q,r})$, $V(t_n,\mathbf{x}_{p,q,r})$ and $\mathbf{A}(t_n,\mathbf{x}_{p,q,r})$, respectively. Furthermore, let Ψ^n, V^n and $\mathbf{A}^n$ be the solution vector at time $t = t_n$ with components $\Psi^n_{p,q,r}$, $V^n_{p,q,r}$ and $\mathbf{A}^n_{p,q,r}$, respectively.

From time $t = t_n$ to $t = t_{n+1}$, we discretize the MD (3.1) and (3.2) as follows: The nonlinear wave-type equations (3.2) are discretized by pseudospectral method for spatial derivatives and then solving the ODEs in phase space analytically under appropriate chosen transmission conditions between different time intervals, and the Dirac equation (3.1) is solved in two splitting steps. For the nonlinear wave-type equations (3.2), we assume

$$V(t,\mathbf{x}) = \sum_{(j,k,l)\in\mathcal{M}} \widetilde{V}^n_{j,k,l}(t)\mathrm{e}^{\mathrm{i}\mu_{j,k,l}\cdot(\mathbf{x}-\mathbf{a})}, \quad \mathbf{x} \in \Omega,\ \ t_n \leqslant t \leqslant t_{n+1}, \tag{3.10}$$

where $\widetilde{f}$ denotes the Fourier coefficients of f and

$$\mathcal{M} = \left\{(j,k,l) \mid -\frac{M_1}{2} \leqslant j < \frac{M_1}{2},\ -\frac{M_2}{2} \leqslant k < \frac{M_2}{2},\ -\frac{M_3}{2} \leqslant l < \frac{M_3}{2}\right\},$$

$$\mu_{j,k,l} = \begin{pmatrix} \mu_j^{(1)} \\ \mu_k^{(2)} \\ \mu_l^{(3)} \end{pmatrix}, \quad \mathbf{a} = \begin{pmatrix} a_1 \\ a_2 \\ a_3 \end{pmatrix}$$

with

$$\mu_j^{(1)} = \frac{2\pi j}{b_1 - a_1}, \quad \mu_k^{(2)} = \frac{2\pi k}{b_2 - a_2}, \quad \mu_l^{(3)} = \frac{2\pi l}{b_3 - a_3}, \quad (j,k,l) \in \mathscr{M}.$$

Plugging (3.10) and (2.8) into (3.2), noticing the orthogonality of the Fourier series, we get the following ODEs for $n \geqslant 0$:

$$\varepsilon^2 \frac{\mathrm{d}^2 \widetilde{V}_{j,k,l}^n(t)}{\mathrm{d}t^2} + |\mu_{j,k,l}|^2 \widetilde{V}_{j,k,l}^n(t) = \widetilde{\rho}_{j,k,l}(t_n) := \widetilde{(|\Psi^n|^2)}_{j,k,l}, \quad t_n \leqslant t \leqslant t_{n+1}, \tag{3.11}$$

$$\widetilde{V}_{j,k,l}^n(t_n) = \begin{cases} \widetilde{(V^{(0)})}_{j,k,l}, & n = 0, \\ \widetilde{V}_{j,k,l}^{n-1}(t_n), & n > 0, \end{cases} \quad (j,k,l) \in \mathscr{M}. \tag{3.12}$$

As noticed in [6], for each fixed $(j,k,l) \in \mathscr{M}$, Eq. (3.11) is a second-order ODE. It needs two initial conditions such that the solution is unique. When $n = 0$ in (3.11) and (3.12), we have the initial condition (3.12) and we can pose the other initial condition for (3.11) due to the initial condition (3.3) for the MD (3.1) and (3.2)

$$\frac{\mathrm{d}}{\mathrm{d}t} \widetilde{V}_{j,k,l}^0(t_0) = \frac{\mathrm{d}}{\mathrm{d}t} \widetilde{V}_{j,k,l}^0(0) = \widetilde{(V^{(1)})}_{j,k,l}. \tag{3.13}$$

Then the solution of (3.11), (3.12) and (3.13) for $t \in [0, t_1]$ is

$$\widetilde{V}_{j,k,l}^0(t) = \begin{cases} \widetilde{(V^{(0)})}_{j,k,l} + t\widetilde{(V^{(1)})}_{j,k,l} + \widetilde{(|\Psi^{(0)}|^2)}_{j,k,l} t^2/2\varepsilon^2, & j = k = l = 0, \\ \left[\widetilde{(V^{(0)})}_{j,k,l} - \widetilde{(|\Psi^{(0)}|^2)}_{j,k,l}/|\mu_{j,k,l}|^2\right] \cos(t|\mu_{j,k,l}|/\varepsilon) & \\ \quad + \widetilde{(V^{(1)})}_{j,k,l} \sin(t|\mu_{j,k,l}|/\varepsilon) \frac{\varepsilon}{|\mu_{j,k,l}|} & \\ \quad + \widetilde{(|\Psi^{(0)}|^2)}_{j,k,l}/|\mu_{j,k,l}|^2 & \text{otherwise.} \end{cases}$$

But when $n > 0$, we only have one initial condition (3.12). One cannot simply pose the continuity between $\frac{\mathrm{d}}{\mathrm{d}t}\widetilde{V}_{j,k,l}^n(t)$ and $\frac{\mathrm{d}}{\mathrm{d}t}\widetilde{V}_{j,k,l}^{n-1}(t)$ across the time $t = t_n$ due to the right-hand side in (3.11) is usually different in two adjacent time intervals $[t_{n-1}, t_n]$ and $[t_n, t_{n+1}]$, i.e. $\widetilde{\rho}_{j,k,l}(t_{n-1}) = \widetilde{(|\Psi^{n-1}|^2)}_{j,k,l} \neq \widetilde{(|\Psi^n|^2)}_{j,k,l} = \widetilde{\rho}_{j,k,l}(t_n)$. Since our goal is to develop explicit scheme and we need linearize the nonlinear term in (3.2) in our discretization (3.11), in general,

$$\frac{\mathrm{d}}{\mathrm{d}t} \widetilde{V}_{j,k,l}^{n-1}(t_n^-) = \lim_{t \to t_n^-} \frac{\mathrm{d}}{\mathrm{d}t} \widetilde{V}_{j,k,l}^{n-1}(t) \neq \lim_{t \to t_n^+} \frac{\mathrm{d}}{\mathrm{d}t} \widetilde{V}_{j,k,l}^n(t) = \frac{\mathrm{d}}{\mathrm{d}t} \widetilde{V}_{j,k,l}^n(t_m^+), \quad n = 1, \ldots \ (j,k,l) \in \mathscr{M}. \tag{3.14}$$

Unfortunately, we do not know the jump $\frac{\mathrm{d}}{\mathrm{d}t}\widetilde{V}_{j,k,l}^n(t_n^+) - \frac{\mathrm{d}}{\mathrm{d}t}\widetilde{V}_{j,k,l}^{n-1}(t_n^-)$ across the time $t = t_n$. In order to get a unique solution of (3.11) and (3.12) for $n > 0$, here we pose an additional condition:

$$\widetilde{V}^n_{j,k,l}(t_{n-1}) = \widetilde{V}^{n-1}_{j,k,l}(t_{n-1}) \quad (j,k,l) \in \mathscr{M}. \tag{3.15}$$

The condition (3.15) is equivalent to pose the solution $\widetilde{V}^n_{j,k,l}(t)$ on the time interval $[t_n, t_{n+1}]$ of (3.11) and (3.12) is also continuity at the time $t = t_{n-1}$. After a simple computation, we get the solution of (3.11), (3.12) and (3.15) for $n > 0$

$$\widetilde{V}^n_{j,k,l}(t) = \begin{cases} \widetilde{V}^n_{j,k,l}(t_n) + \widetilde{\rho}_{j,k,l}(t_n)(t-t_n)^2/2\varepsilon^2 \\ \quad + \frac{t-t_n}{\Delta t}\left[\widetilde{V}^n_{j,k,l}(t_n) - \widetilde{V}^{n-1}_{j,k,l}(t_{n-1}) + \widetilde{\rho}_{j,k,l}(t_n)(\Delta t)^2/2\varepsilon^2\right], & j=k=l=0, \\ \left[\widetilde{V}^n_{j,k,l} - \widetilde{\rho}_{j,k,l}(t_n)/|\mu_{j,k,l}|^2\right]\cos((t-t_n)|\mu_{j,k,l}|/\varepsilon) \\ \quad + \Big[(1-\cos(|\mu_{j,k,l}|\Delta t/\varepsilon))\widetilde{\rho}_{j,k,l}(t_n)/|\mu_{j,k,l}|^2 - \widetilde{V}^{n-1}_{j,k,l}(t_{n-1}) \\ \quad + \widetilde{V}^n_{j,k,l}(t_n)\cos(|\mu_{j,k,l}|\Delta t/\varepsilon)\Big]\frac{\sin((t-t_n)|\mu_{j,k,l}|/\varepsilon)}{\sin(|\mu_{j,k,l}|\Delta t/\varepsilon)} \\ \quad + \widetilde{\rho}_{j,k,l}(t_n)/|\mu_{j,k,l}|^2 & \text{otherwise.} \end{cases}$$

Discretization for the equation of $\mathbf{A}$ in (3.2) can be done in a similar way.

For the Dirac equation (3.1), we solve it in two splitting steps. One solves first

$$\mathrm{i}\delta\partial_t \Psi(t,\mathbf{x}) = -\mathrm{i}\frac{\delta}{\varepsilon}\sum_{k=1}^{3}\alpha^k\partial_k\Psi + \frac{1}{\varepsilon^2}\beta\Psi, \quad \mathbf{x}\in\Omega, \ \ t_n \leqslant t \leqslant t_{n+1} \tag{3.16}$$

for the time step of length Δt, followed by solving

$$\mathrm{i}\delta\partial_t \Psi(t,\mathbf{x}) = (V + V^{\mathrm{ext}})\Psi - \sum_{k=1}^{3}\alpha^k(A_k + A_k^{\mathrm{ext}})\Psi = G(t,\mathbf{x})\Psi \tag{3.17}$$

for the same time step with

$$G(t,\mathbf{x}) = \left[(V(t,\mathbf{x}) + V^{\mathrm{ext}}(t,\mathbf{x}))\mathbb{I}_4 - \sum_{k=1}^{3}\alpha^k\big(A_k(t,\mathbf{x}) + A_k^{\mathrm{ext}}(t,\mathbf{x})\big)\right]. \tag{3.18}$$

For each fixed $\mathbf{x}\in\Omega$, integrating (3.17) from t_n to t_{n+1}, and then approximating the integral on $[t_n, t_{n+1}]$ via the Simpson rule, one reads

$$\begin{aligned} \Psi(t_{n+1},\mathbf{x}) &= \exp\left[-\mathrm{i}\frac{1}{\delta}\int_{t_n}^{t_{n+1}} G(t,\mathbf{x})\,\mathrm{d}t\right]\Psi(t_n,\mathbf{x}) \\ &\approx \exp\left[-\mathrm{i}\frac{\Delta t}{\delta}\big(G(t_n,\mathbf{x}) + 4G(t_{n+1/2},\mathbf{x}) + G(t_{n+1},\mathbf{x})\big)/6\right]\Psi(t_n,\mathbf{x}) \\ &= \exp\left[-\mathrm{i}\frac{\Delta t}{\delta}G^{n+1/2}(\mathbf{x})\right]\Psi(t_n,\mathbf{x}). \end{aligned} \tag{3.19}$$

Since $G^{n+1/2}(\mathbf{x})$ is a U-matrix, i.e. $(\bar{G}^{n+1/2}(\mathbf{x}))^{\mathrm{T}} = G^{n+1/2}(\mathbf{x})$, it is diagonalizable (see detail in Appendix A), i.e. there exist a diagonal matrix $D^{n+1/2}(\mathbf{x})$ and a complex orthogonormal matrix $P^{n+1/2}(\mathbf{x})$, i.e. $(\bar{P}^{n+1/2}(\mathbf{x}))^{\mathrm{T}} = (P^{n+1/2}(\mathbf{x}))^{-1}$, such that

$$G^{n+1/2}(\mathbf{x}) = P^{n+1/2}(\mathbf{x})D^{n+1/2}(\mathbf{x})(\bar{P}^{n+1/2}(\mathbf{x}))^{\mathrm{T}}, \quad \mathbf{x}\in\Omega. \tag{3.20}$$

Plugging (3.20) into (3.19), we obtain

$$\Psi(t_{n+1},\mathbf{x}) = P^{n+1/2}(\mathbf{x})\exp\left[-\mathrm{i}\frac{\Delta t}{\delta}D^{n+1/2}(\mathbf{x})\right](\bar{P}^{n+1/2}(\mathbf{x}))^{\mathrm{T}}\Psi(t_n,\mathbf{x}),\quad \mathbf{x}\in\Omega. \tag{3.21}$$

For discretizing (3.16), we assume

$$\Psi(t,\mathbf{x}) = \sum_{(j,k,l)\in\mathscr{M}}\widetilde{\Psi}_{j,k,l}(t)\mathrm{e}^{\mathrm{i}\mu_{j,k,l}\cdot(\mathbf{x}-\mathbf{a})},\quad \mathbf{x}\in\Omega,\ \ t_n\leqslant t\leqslant t_{n+1}. \tag{3.22}$$

Substituting (3.22) into (3.16), we have

$$\frac{\mathrm{d}\widetilde{\Psi}_{j,k,l}(t)}{\mathrm{d}t} = -\frac{\mathrm{i}}{\varepsilon}M_{j,k,l}\widetilde{\Psi}_{j,k,l}(t),\quad t_n\leqslant t\leqslant t_{n+1}\ \ (j,k,l)\in\mathscr{M}, \tag{3.23}$$

where the matrix

$$M_{j,k,l} = \mu_j^{(1)}\alpha^1 + \mu_k^{(2)}\alpha^2 + \mu_l^{(3)}\alpha^3 + \varepsilon^{-1}\delta^{-1}. \tag{3.24}$$

Since $M_{j,k,l}$ is a U-matrix, again it is diagonalizable (see detail in Appendix B), i.e. there exist a diagonal matrix $D_{j,k,l}$ and a complex orthogonormal matrix $P_{j,k,l}$ such that

$$M_{j,k,l} = P_{j,k,l}D_{j,k,l}(\bar{P}_{j,k,l})^{\mathrm{T}}\quad (j,k,l)\in\mathscr{M}. \tag{3.25}$$

Thus the solution of (3.23) is

$$\begin{aligned}\widetilde{\Psi}_{j,k,l}(t) &= \exp\left[-\frac{\mathrm{i}}{\varepsilon}(t-t_n)M_{j,k,l}\right]\widetilde{\Psi}_{j,k,l}(t_n)\\ &= P_{j,k,l}\exp\left[-\frac{\mathrm{i}}{\varepsilon}(t-t_n)D_{j,k,l}\right](\bar{P}_{j,k,l})^{\mathrm{T}}\widetilde{\Psi}_{j,k,l}(t_n),\quad t_n\leqslant t\leqslant t_{n+1}.\end{aligned} \tag{3.26}$$

From time $t=t_n$ to $t=t_{n+1}$, we combine the splitting steps via the standard Strang splitting:

$$V_{p,q,r}^{n+1} = \sum_{(j,k,l)\in\mathscr{M}}\widetilde{V}_{j,k,l}^{n}(t_{n+1})\mathrm{e}^{\mathrm{i}\mu_{j,k,l}\cdot(\mathbf{x}_{p,q,r}-\mathbf{a})}, \tag{3.27}$$

$$\mathbf{A}_{p,q,r}^{n+1} = \sum_{(j,k,l)\in\mathscr{M}}\widetilde{\mathbf{A}}_{j,k,l}^{n}(t_{n+1})\mathrm{e}^{\mathrm{i}\mu_{j,k,l}\cdot(\mathbf{x}_{p,q,r}-\mathbf{a})}\quad (p,q,r)\in\mathscr{N}, \tag{3.28}$$

$$\begin{aligned}\Psi_{p,q,r}^{*} &= \sum_{(j,k,l)\in\mathscr{M}}P_{j,k,l}\exp\left[-\frac{\mathrm{i}\Delta t}{2\varepsilon}D_{j,k,l}\right](\bar{P}_{j,k,l})^{\mathrm{T}}\widetilde{(\Psi^{n})}_{j,k,l}\mathrm{e}^{\mathrm{i}\mu_{j,k,l}\cdot(\mathbf{x}_{p,q,r}-\mathbf{a})},\\ \Psi_{p,q,r}^{**} &= P^{n+1/2}(\mathbf{x}_{p,q,r})\exp\left[-\mathrm{i}\frac{\Delta t}{\delta}D^{n+1/2}(\mathbf{x}_{p,q,r})\right](\bar{P}^{n+1/2}(\mathbf{x}_{p,q,r}))^{\mathrm{T}}\Psi_{p,q,r}^{*},\\ \Psi_{p,q,r}^{n+1} &= \sum_{(j,k,l)\in\mathscr{M}}P_{j,k,l}\exp\left[-\frac{\mathrm{i}\Delta t}{2\varepsilon}D_{j,k,l}\right](\bar{P}_{j,k,l})^{\mathrm{T}}\widetilde{(\Psi^{**})}_{j,k,l}\mathrm{e}^{\mathrm{i}\mu_{j,k,l}\cdot(\mathbf{x}_{p,q,r}-\mathbf{a})},\end{aligned} \tag{3.29}$$

where the formula for $\widetilde{V}_{j,k,l}^{n}(t_{n+1})$ and $\widetilde{\mathbf{A}}_{j,k,l}^{n}(t_{n+1})$ are given in Appendix C and $\widetilde{U}_{j,k,l}$ the discrete Fourier transform coefficients of the vector $\{U_{p,q,r},(p,q,r)\in\mathscr{N}\}$ are defined as

$$\widetilde{U}_{j,k,l} = \frac{1}{M_1 M_2 M_3} \sum_{(p,q,r)\in\mathcal{Q}} U_{p,q,r} \mathrm{e}^{\mathrm{i}\mu_{j,k,l}\cdot(\mathbf{x}_{p,q,r}-\mathbf{a})} \quad (j,k,l)\in\mathcal{M}, \tag{3.30}$$

where

$$\mathcal{Q} = \{(p,q,r) \mid 0 \leqslant p \leqslant M_1 - 1,\ 0 \leqslant q \leqslant M_2 - 1,\ 0 \leqslant r \leqslant M_3 - 1\}.$$

The initial conditions (3.3) and (3.4) are discretized as

$$\Psi^0_{p,q,r} = \Psi^{(0)}(\mathbf{x}_{p,q,r}), \quad V^0_{p,q,r} = V^{(0)}(\mathbf{x}_{p,q,r}), \quad \frac{\mathrm{d}V^0_{p,q,r}(0)}{\mathrm{d}t} = V^{(1)}(\mathbf{x}_{p,q,r}), \quad \mathbf{A}^0_{p,q,r} = \mathbf{A}^{(0)}(\mathbf{x}_{p,q,r}),$$
$$\frac{\mathrm{d}\mathbf{A}^0_{p,q,r}(0)}{\mathrm{d}t} = \mathbf{A}^{(1)}(\mathbf{x}_{p,q,r}), \quad (p,q,r)\in\mathcal{N}.$$

Remark 3.1. We use the Simpson quadrature rule to approximate the integration in (3.19) instead of the trapezodial rule which was used in [6,7] for a similar integration. The reason is that we want the quadrature is exact when the MD system (2.5) and (2.6) admits the plane wave solution (2.23)–(2.25). In this case, the integrand $G(t,\mathbf{x})$ is quadratic in t. Thus the algorithm (3.27)–(3.29) gives exact results when the MD system admits plane wave solution.

3.2. Properties of the numerical method

1. *Plane wave solution*: If the initial data in (3.3) and (3.4) are chosen as in (2.20)–(2.22), and the external electric and magnetic fields, i.e. V^{ext} and $\mathbf{A}^{\mathrm{ext}}$, are chosen as in (2.24) and (2.25), then the MD system (3.1)–(3.5) admits the plane wave solution (2.23)–(2.25). It is easy to see that in this case our numerical method (3.27)–(3.29) gives exact results provided that $M_j \geqslant 2(|\omega_j| + 1)$ $(j = 1,2,3)$.

2. *Time transverse invariant*: If constants α_0 and α_1 are added to $V^{(0)}$ and $V^{(1)}$, respectively, in (3.3), then the solution V^n get added by $\alpha_0 + \alpha_1 t_n$ and Ψ^n get multiplied by $e^{-it_n(\alpha_0+\alpha_1 t_n/2)/\delta}$, which leaves density of each particle $|\psi^n_j|$ $(j = 1,2,3,4)$ unchanged.

3. *Conservation*: Let $\mathbf{U} = \{U_{p,q,r}, (p,q,r)\in\mathcal{N}\}$ and $f(\mathbf{x})$ a periodic function on the box Ω, and let $\|\cdot\|_{l^2}$ be the usual discrete l^2-norm on the box Ω, i.e.

$$\|\mathbf{U}\|^2_{l^2} = h_1 h_2 h_3 \sum_{(p,q,r)\in\mathcal{Q}} |U_{p,q,r}|^2, \tag{3.31}$$

$$\mathrm{DMean}(\mathbf{U}) = h_1 h_2 h_3 \sum_{(p,q,r)\in\mathcal{Q}} U_{p,q,r}, \tag{3.32}$$

$$\|f\|^2_{l^2} = h_1 h_2 h_3 \sum_{(p,q,r)\in\mathcal{Q}} |f(\mathbf{x}_{p,q,r})|^2. \tag{3.33}$$

Then we have:

Theorem 3.1. *The time splitting spectral method* (3.27)–(3.29) *for the MD conserves the following quantities in the discretized level:*

$$\|\Psi^n\|_{l^2} = \|\Psi^0\|_{l^2} = \|\Psi^{(0)}\|_{l^2}, \quad n = 0,1,2,\ldots, \tag{3.34}$$

$$\mathrm{DMean}(V^n) = \mathrm{DMean}(V^{(0)}) + t_n \mathrm{DMean}(V^{(1)}) + \frac{t_n^2}{2\varepsilon^2}\mathrm{DMean}(|\Psi^{(0)}|^2). \tag{3.35}$$

Proof. See Appendix D. □

4. *Unconditional stability*: By the standard Von Neumann analysis for (3.27) and (3.28), noting (3.34), we get the method (3.27)–(3.29) is unconditionally stable. In fact, setting $\Psi^n = \mathbf{0}$ and plugging $\tilde{V}^n_{j,k,l}(t_{n+1}) = \mu \tilde{V}^n_{j,k,l}(t_n) = \mu^2 \tilde{V}^{n-1}_{j,k,l}(t_{n-1})$ into (C.3) with $|\mu|$ the amplification factor, we obtain the characteristic equation:

$$\mu^2 - 2\mu\cos(|\mu_{j,k,l}|\Delta t/\varepsilon) + 1 = 0, \quad (j,k,l) \in \mathscr{M}. \tag{3.36}$$

This implies

$$\mu = \cos(|\mu_{j,k,l}|\Delta t/\varepsilon) \pm \mathrm{i}\sin(|\mu_{j,k,l}|\Delta t/\varepsilon). \tag{3.37}$$

Thus the amplification factor

$$G_{j,k,l} = |\mu| = \sqrt{\cos^2(|\mu_{j,k,l}|\Delta t/\varepsilon) + \sin^2(|\mu_{j,k,l}|\Delta t/\varepsilon)} = 1 \quad (j,k,l) \in \mathscr{M}. \tag{3.38}$$

Similar results can be obtained for (3.28). These together with (3.34) imply the method (3.27)–(3.29) is unconditionally stable. This is confirmed by our numerical results in the next section.

5. *ε-resolution in the 'nonrelatistic' limit regime* ($0 < \varepsilon \ll 1$): As our numerical results in the next section suggest: The meshing strategy (or ε-resolution) which guarantees 'good' numerical results in the 'nonrelatistic' limit regime, i.e. $0 < \varepsilon \ll 1$, is

$$h = \max\{h_1, h_2, h_3\} = \mathrm{O}(\varepsilon), \quad \Delta t = \mathrm{O}(\varepsilon^2). \tag{3.39}$$

3.3. For homogeneous Dirichlet boundary conditions

In some cases, the periodic boundary conditions (3.5) may be replaced by the following homogeneous Dirichlet boundary conditions:

$$\Psi(t,\mathbf{x}) = V(t,\mathbf{x}) = 0, \quad \mathbf{A}(t,\mathbf{x}) = \mathbf{0}, \quad \mathbf{x} \in \partial\Omega, \ \ t \geqslant 0. \tag{3.40}$$

In this case, the method designed above is still valid provided that we replace the Fourier basis functions by sine basis functions. Let

$$\mathscr{M} = \{(j,k,l) \mid 1 \leqslant j \leqslant M_1 - 1, \ 1 \leqslant k \leqslant M_2 - 1, \ 1 \leqslant l \leqslant M_3 - 1\},$$

$$\mu_j^{(1)} = \frac{\pi j}{b_1 - a_1}, \quad \mu_k^{(2)} = \frac{\pi k}{b_2 - a_2}, \quad \mu_l^{(3)} = \frac{\pi l}{b_3 - a_3} \quad (j,k,l) \in \mathscr{M}. \tag{3.41}$$

The detailed scheme is:

$$V^{n+1}_{p,q,r} = \sum_{(j,k,l)\in\mathscr{M}} \widetilde{V}^{n}_{j,k,l}(t_{n+1}) \sin\left(\frac{pj\pi}{M_1}\right)\sin\left(\frac{qk\pi}{M_2}\right)\sin\left(\frac{rl\pi}{M_3}\right),$$

$$\mathbf{A}^{n+1}_{p,q,r} = \sum_{(j,k,l)\in\mathscr{M}} \widetilde{\mathbf{A}}^{n}_{j,k,l}(t_{n+1}) \sin\left(\frac{pj\pi}{M_1}\right)\sin\left(\frac{qk\pi}{M_2}\right)\sin\left(\frac{rl\pi}{M_3}\right) \quad (p,q,r)\in\mathscr{M},$$

$$\Psi^{*}_{p,q,r} = \sum_{(j,k,l)\in\mathscr{M}} P_{j,k,l}\exp\left[-\frac{i\Delta t}{2\varepsilon}D_{j,k,l}\right](\bar{P}_{j,k,l})^{\mathrm{T}}(\widetilde{\Psi^{n}})_{j,k,l}\sin\left(\frac{pj\pi}{M_1}\right)\sin\left(\frac{qk\pi}{M_2}\right)\sin\left(\frac{rl\pi}{M_3}\right),$$

$$\Psi^{**}_{p,q,r} = P^{n+1/2}(\mathbf{x}_{p,q,r})\exp\left[-\mathrm{i}\frac{\Delta t}{\delta}D^{n+1/2}(\mathbf{x}_{p,q,r})\right](\bar{P}^{n+1/2}(\mathbf{x}_{p,q,r}))^{\mathrm{T}}\Psi^{*}_{p,q,r},$$

$$\Psi^{n+1}_{p,q,r} = \sum_{(j,k,l)\in\mathscr{M}} P_{j,k,l}\exp\left[-\frac{\mathrm{i}\Delta t}{2\varepsilon}D_{j,k,l}\right](\bar{P}_{j,k,l})^{\mathrm{T}}(\widetilde{\Psi^{**}})_{j,k,l}\sin\left(\frac{pj\pi}{M_1}\right)\sin\left(\frac{qk\pi}{M_2}\right)\sin\left(\frac{rl\pi}{M_3}\right),$$

where the formula for $\widetilde{V}^{n}_{j,k,l}(t_{n+1})$ and $\widetilde{\mathbf{A}}^{n}_{j,k,l}(t_{n+1})$ are given in Appendix C with $\mu_{j,k,l}$ is replaced by (3.41), and $\widetilde{U}_{j,k,l}$ the discrete sine transform coefficients of the vector $\{U_{p,q,r},(p,q,r)\in\mathscr{N}\}$ are defined as

$$\widetilde{U}_{j,k,l} = \frac{8}{M_1M_2M_3}\sum_{(p,q,r)\in\mathscr{M}} U_{p,q,r}\sin\left(\frac{pj\pi}{M_1}\right)\sin\left(\frac{qk\pi}{M_2}\right)\sin\left(\frac{rl\pi}{M_3}\right), \quad (j,k,l)\in\mathscr{M}. \tag{3.42}$$

4. Numerical results

In this section, we present numerical results to demonstrate 'good' properties of our numerical method for MD and apply it to study dynamics of MD.

In Examples 1 and 3, the initial data in (3.3) and (3.4) are chosen as

$$\psi^{(0)}_{j}(\mathbf{x}) = \frac{(\gamma_1\gamma_2\gamma_3)^{1/4}}{2\pi^{3/4}}\exp[-(\gamma_1x_1^2+\gamma_2x_2^2+\gamma_3x_3^2)/2)\exp(\mathrm{i}c_jx_1/\varepsilon), \tag{4.1}$$

$$V^{(0)}(\mathbf{x}) = 0, \quad V^{(1)}(\mathbf{x}) = 0, \quad \mathbf{A}^{(0)}(\mathbf{x}) = \mathbf{0}, \quad \mathbf{x}\in\mathbb{R}^3. \tag{4.2}$$

They, together with $\mathbf{A}^{(1)}$, decay to zero sufficient fast as $|\mathbf{x}|\to\infty$. This Gaussian-type initial data is often used to study wave motion and interaction in physical literatures. We always compute on a box, which is large enough such that the periodic boundary conditions (3.5) do not introduce a significant aliasing error relative to the problem in the whole space. In our computations, we always choose uniform mesh, i.e. $h = h_1 = h_2 = h_3$.

4.1. Numerical accuracy

Example 1. Accuracy test and meshing strategy, i.e. we choose $\delta = 1$, $V^{\mathrm{ext}}(t,\mathbf{x})\equiv 0$, $\mathbf{A}^{\mathrm{ext}}(t,\mathbf{x})\equiv\mathbf{0}$ in (3.1), $\gamma_1=\gamma_2=\gamma_3=5$ and $c_1=c_2=c_3=c_4=1$ in (4.1) and $\mathbf{A}^{(1)}(\mathbf{x})=\mathbf{0}$ in (3.4).

We solve the MD (3.1)–(3.5) on a box $\Omega=[-4,4]^3$ by using our numerical method (3.27)–(3.29), and present results for two different regimes of velocity, i.e. $1/\varepsilon$:

Case I. O(1)-velocity speed, i.e. we choose $\varepsilon = 1$ in (3.1), (3.2) and (4.1). Here we test the spatial and temporal discretization errors. Let Ψ, V and $\mathbf{A}$ be the 'exact' solutions which are obtained numerically by

using our numerical method with a very fine mesh and time step, e.g. $h = \frac{1}{8}$ and $\Delta t = 0.0001$, and $\Psi^{h,\Delta t}$, $V^{h,\Delta t}$ and $\mathbf{A}^{h,\Delta t}$ be the numerical solution obtained by using our method with mesh size h and time step Δt. To quantify the numerical method, we define the error functions as

$$e_\Psi(t) = \|\Psi(t,\cdot) - \Psi^{h,\Delta t}(t,\cdot)\|_{l^2}, \quad e_{\mathbf{A}}(t) = \|\mathbf{A}(t,\cdot) - \mathbf{A}^{h,\Delta t}(t,\cdot)\|_{l^2}, \quad e_V(t) = \|V(t,\cdot) - V^{h,\Delta t}(t,\cdot)\|_{l^2}.$$

First, we test the discretization error in space. In order to do this, we choose a very small time step, e.g. $\Delta t = 0.0001$, such that the error from time discretization is negligible comparing to the spatial discretization error. Table 1 lists the numerical errors of $e_\Psi(t)$, $e_V(t)$ and $e_{\mathbf{A}}(t)$ at $t = 0.4$ with different mesh sizes h.

Second, we test the discretization error in time. Table 2 shows the numerical errors of $e_\Psi(t)$, $e_V(t)$ and $e_{\mathbf{A}}(t)$ at $t = 0.4$ under different time step Δt and mesh size $h = 1/4$.

Third, we test the density conservation in (3.34). Table 3 shows $\|\Psi\|_{l^2}$ at different times.

Case II: 'nonrelativistic' limit regime, i.e. $0 < \varepsilon \ll 1$. Here we test the ε-resolution of our numerical method. Fig. 1 shows the numerical results at $t = 0.4$ when we choose the meshing strategy: $\varepsilon = 1$, $h = 1/2$, $\Delta t = 0.2$; $\varepsilon = 1/2$, $h = 1/4$, $\Delta t = 0.05$; $\varepsilon = 1/4$, $h = 1/8$, $\Delta t = 0.0125$; which corresponds to meshing strategy $h = \mathrm{O}(\varepsilon)$, $\Delta t = \mathrm{O}(\varepsilon^2)$.

From Tables 1–3 and Fig. 1, we can draw the following observations:

Our numerical method for MD is of spectral order accuracy in space and second order accuracy in time, and conserves the density up to 12-digits. In the 'nonrelativistic' limit regime, i.e. $0 < \varepsilon \ll 1$, the ε-resolution is: $h = \mathrm{O}(\varepsilon)$ and $\Delta t = \mathrm{O}(\varepsilon^2)$. Furthermore, our additional numerical experiments confirm that the method is unconditionally stable, and show that meshing strategy: $h = O(\varepsilon)$ and $\Delta t = O(\varepsilon)$ gives 'incorrect' numerical results in 'nonrelativistic' limit regime.

Table 1
Spatial discretization error analysis: at time $t = 0.4$ under $\Delta t = 0.0001$

Mesh	$h = 1$	$h = 0.5$	$h = 0.25$	$h = 0.125$
$e_\Psi(t)$	0.76250	$5.8928E-2$	$7.7029E-6$	$2.2164E-11$
$e_V(t)$	$6.4937E-3$	$3.9210E-4$	$8.8440E-5$	$7.6842E-13$
$e_{\mathbf{A}}(t)$	$7.0499E-3$	$4.6114E-4$	$1.1609E-6$	$7.6508E-13$

Table 2
Temporal discretization error analysis: at time $t = 0.4$ under $h = 1/4$

Time step	$\Delta t = 0.05$	$\Delta t = 0.025$	$\Delta t = 0.0125$	$\Delta t = 0.00625$
$e_\Psi(t)$	$7.7643E-5$	$1.9592E-5$	$4.9041E-6$	$1.2063E-6$
$e_V(t)$	$2.9906E-4$	$7.4114E-5$	$1.8405E-5$	$4.5103E-6$
$e_{\mathbf{A}}(t)$	$3.5809E-4$	$8.8633E-5$	$2.2004E-5$	$5.381E-6$

Table 3
Density conservation test

Time	$t = 0$	$t = 1$	$t = 2$
$\|\Psi(t,\cdot)\|_{l^2}$	0.9999999999999	0.9999999999998	0.9999999999996

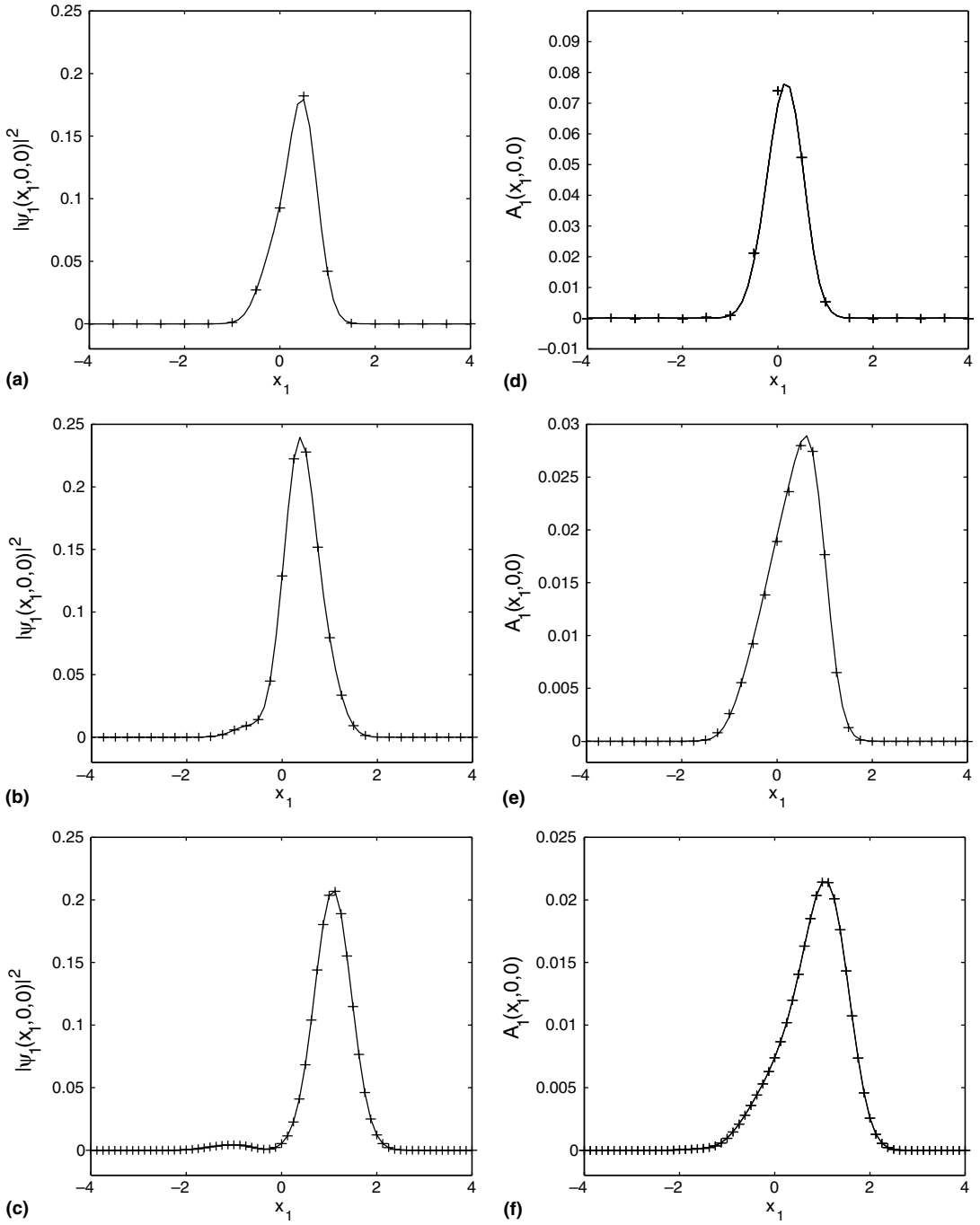

Fig. 1. Meshing strategy test in Example 1 for wave function $|\Psi_1(t,x_1,0,0)|^2$ (left column) and magnetic potential $A_1(t,x_1,0,0)$ (right column) at time $t = 0.4$. (–) 'exact' solutions; (+++) numerical solutions. (a) & (d) $\varepsilon = 1$, $h = 1$ and $\Delta t = 0.2$; (b) & (e) $\varepsilon = 1/2$, $h = 1/2$ and $\Delta t = 0.05$; (c) & (f) $\varepsilon = 1/4$, $h = 1/4$ and $\Delta t = 0.0125$; which corresponds to meshing strategy: $h = \mathrm{O}(\varepsilon)$ and $\Delta t = \mathrm{O}(\varepsilon^2)$.

4.2. Applications

Example 2. Exact results for plane wave solution of free MD, i.e. we choose $\varepsilon = 1$, $\delta = 12.97$ in (3.1), (3.2). The external electromagnetic potentials are chosen as in (2.24), and the initial data is taken as in (2.20)–(2.22) with $\omega_1 = 3, \omega_2 = \omega_3 = 5$, $V^{(0)} = 1/\pi^2$, $V^{(1)} = -1/2\pi^3$, $\mathbf{A}^{(0)} = \mathbf{0}$ and $\mathbf{A}^{(1)} = (0, -1/7\pi^2, 0)^{\mathrm{T}}$. Thus the plane wave solution of free MD is given in (2.23)–(2.25)

We solve (3.1)–(3.5) on $\Omega = [-\pi, \pi]^3$ by our numerical method (3.27)–(3.29) with $h = \pi/8$ and time step $\Delta t = 0.01$. Fig. 2 shows the numerical results at different times.

From Fig. 2, we can see that our method really gives exact results for plane wave solution of free MD.

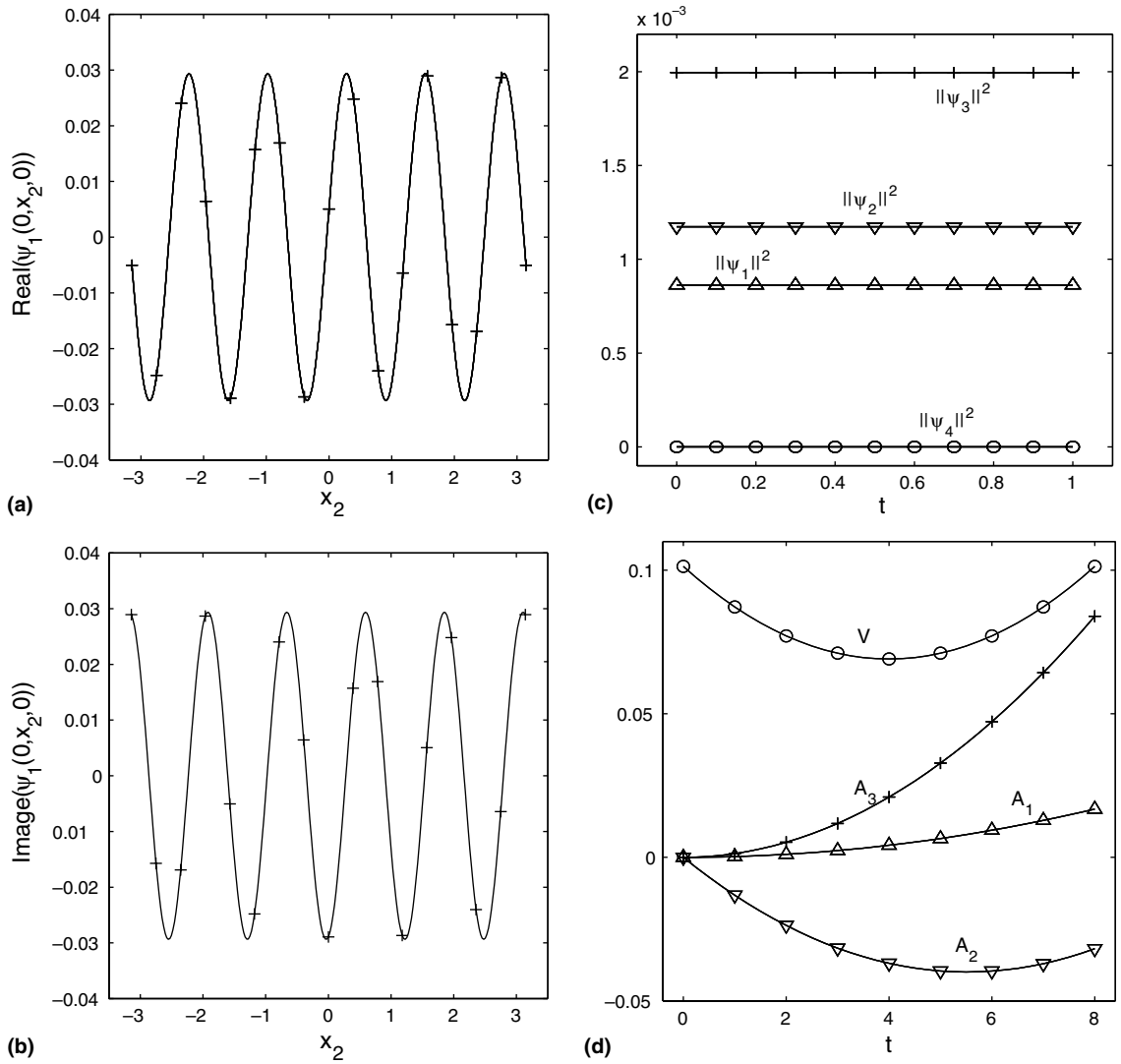

Fig. 2. Numerical results for Example 2 of wave function $\Psi_1(t, 0, x_2, 0)$ (left column) at $t = 1.0$, time-evolution of position density and electromagnetic potentials (right column). (–) exact solutions; (+++) numerical solutions.

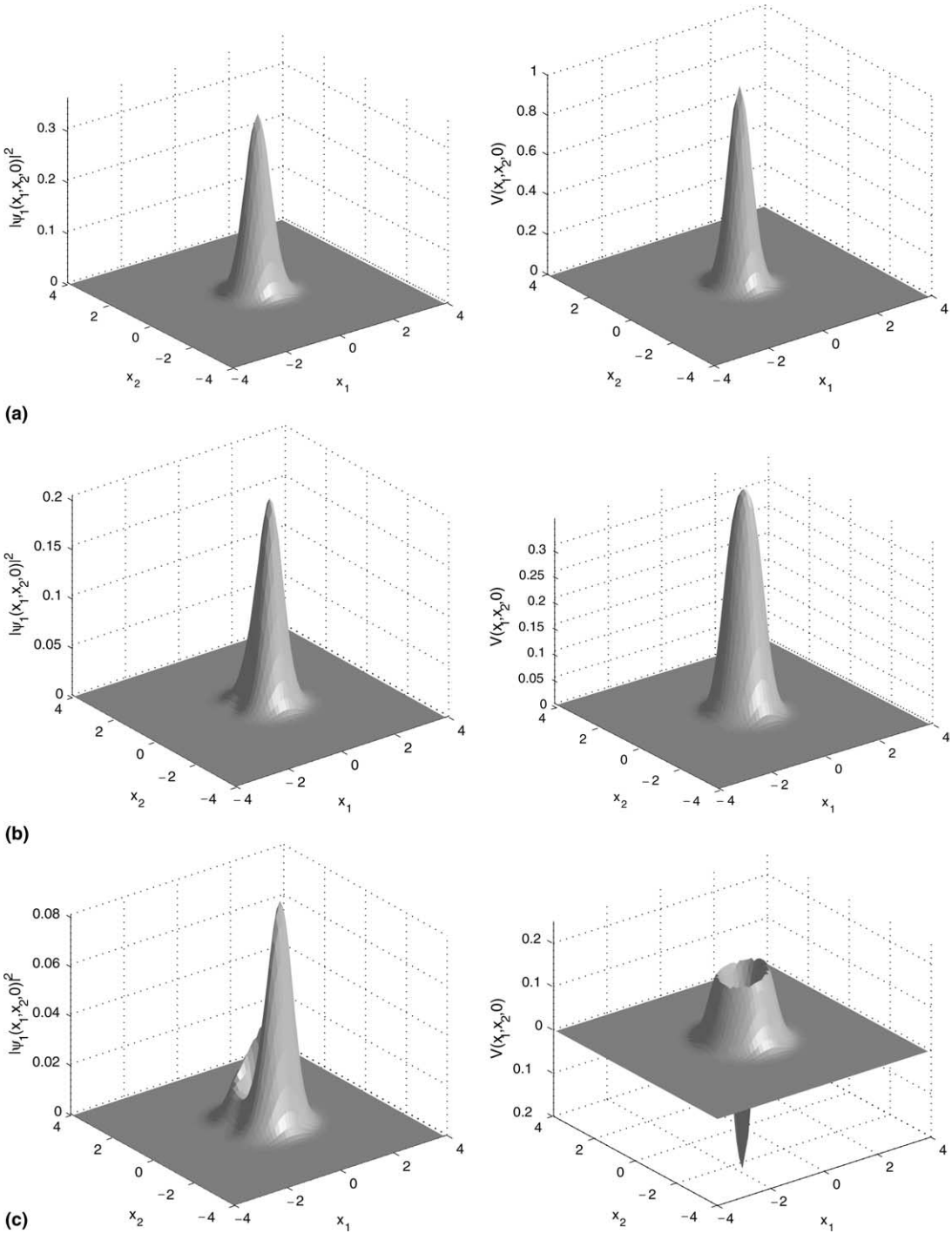

Fig. 3. Surface plots of the wave function $|\Psi_1(t,x_1,x_2,0)|^2$ (left column) and electro potential $V(t,x_1,x_2,0)$ (right column) at different times in Example 3 for Case 1. (a) $t = 0$, (b) $t = 0.25$, (c) $t = 0.5$.

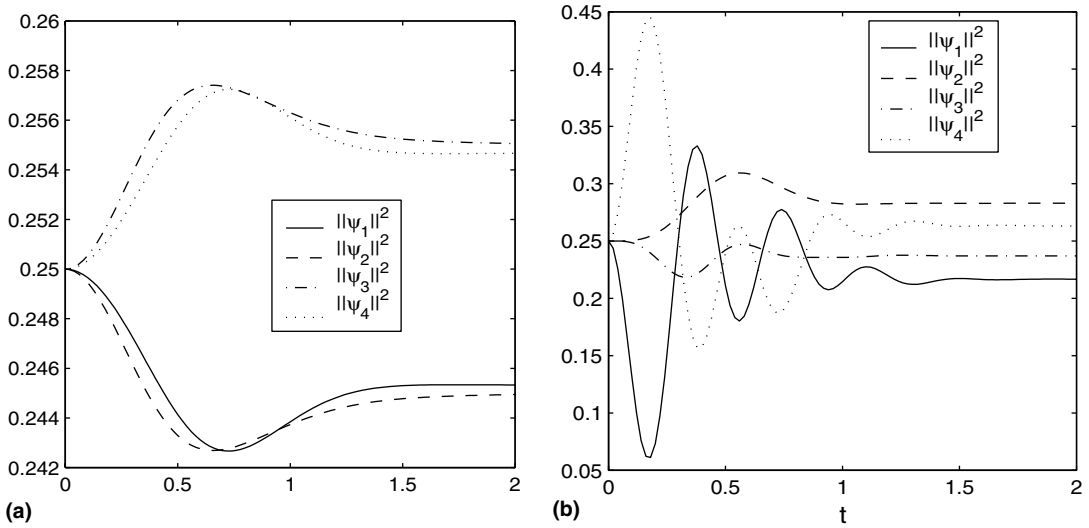

Fig. 4. Time-evolution of position densities in Example 3. (a) Case 1; (b) Case 2.

Example 3. Dynamics of MD, i.e. we choose $\varepsilon = 1$, $\delta = 10.9149$, $V^{\text{ext}}(t, \mathbf{x}) \equiv 0$, $\mathbf{A}^{\text{ext}}(t, \mathbf{x}) \equiv \mathbf{0}$ in (3.1) and (3.2), and $A_k^{(1)}(\mathbf{x}) = \mathrm{e}^{-4(x_1^2+x_2^2+x_3^2)}$ $(1 \leqslant k \leqslant 3)$ in (3.4).

We present results for two sets of parameters in (4.1):

Case 1: $\gamma_1 = 3$, $\gamma_2 = 4$, $\gamma_3 = 5$, $c_1 = c_2 = c_3 = c_4 = -1$,

Case 2: $\gamma_1 = 2$, $\gamma_2 = 4$, $\gamma_3 = 8$, $c_1 = 8$, $c_2 = 4$,$c_3 = -4$, $c_4 = 1$.

We solve this problem on a box $[-8, 8]^3$ by our method with mesh size $h = 1/8$ and time step $\Delta t = 0.002$. Fig. 3 shows the surfaces plots of $|\Psi_1(t, x_1, x_2, 0)|^2$ and $V(t, x_1, x_2, 0)$ at different times for Case 1. Fig. 4 shows time-evolution of particle densities $\|\Psi_j(t, \cdot)\|^2$ $(j = 1, 2, 3, 4)$ for Cases 1 and 2.

From Fig. 4, we can see that the total density $\|\Psi\|^2$ is conserved in the two cases. In case 1, the density for the first two components decreases for a period, attains their minimum, and then increases; where the time-evolution of the density for the other two components is in an opposite way in order to keep the conservation of the total density. Similar time-evolution pattern of density is formed in case 2 except more oscillation due to the nonuniform initial phase in the wave-function (cf. (4.1)). An interesting phenomenon in Fig. 4 is that after some time period, the density for each component almost keeps as a constant, i.e. there is no mass exchange between different components.

5. Conclusion

An explicit, unconditionally stable and accurate time-splitting spectral method (TSSP) is designed for the Maxwell–Dirac system (MD). The method is explicit, unconditionally stable, time reversible, time transverse invariant, and of spectral-order accuracy in space and second-order accuracy in time. Moreover, it conserves the total position density exactly in discretized level and gives exact results for plane wave solution of free MD. Extensive numerical tests are presented to confirm the above properties of the numerical method. Our numerical tests also suggest the following meshing strategy (or ε-resolution) is admissible in the 'nonrelativistic' limit regime $(0 < \varepsilon \ll 1)$: spatial mesh size $h = \mathrm{O}(\varepsilon)$ and time step $\triangle t = \mathrm{O}(\varepsilon^2)$. The method is also applied to study dynamics of MD. In the future, we plan to use this state-of-the-art

numerical method to study more complicated time-evolution of fast (relativistic) electrons and positrons within external and self-generated electromagnetic fields.

Acknowledgements

The authors acknowledge support by the National University of Singapore Grant No. R-151-000-027-112 and thank very helpful discussions with Peter Markowich and Christof Sparber.

Appendix A. Diagnolize the matrix $G^{n+1/2}(\mathrm{x})$ in (3.19) and computation

From (3.19), notice (3.18), we have

$$G^{n+1/2}(\mathbf{x}) = \frac{1}{6}\left[G(t_n,\mathbf{x}) + 4G(t_{n+1/2},\mathbf{x}) + G(t_{n+1},\mathbf{x})\right] = \begin{pmatrix} V^{n+1/2}(\mathbf{x}) & 0 & -A_3^{n+1/2}(\mathbf{x}) & -A_-^{n+1/2}(\mathbf{x}) \\ 0 & V^{n+1/2}(\mathbf{x}) & -A_+^{n+1/2}(\mathbf{x}) & A_3^{n+1/2}(\mathbf{x}) \\ -A_3^{n+1/2}(\mathbf{x}) & -A_-^{n+1/2}(\mathbf{x}) & V^{n+1/2}(\mathbf{x}) & 0 \\ -A_+^{n+1/2}(\mathbf{x}) & A_3^{n+1/2}(\mathbf{x}) & 0 & V^{n+1/2}(\mathbf{x}) \end{pmatrix} \tag{A.1}$$

with

$$\begin{aligned} A_\pm^{n+1/2}(\mathbf{x}) &= A_1^{n+1/2}(\mathbf{x}) \pm \mathrm{i}A_2^{n+1/2}(\mathbf{x}), \\ V^{n+1/2}(\mathbf{x}) &= \frac{1}{6}\left[V(t_n,\mathbf{x}) + V^{\mathrm{ext}}(t_n,\mathbf{x}) + 4(V(t_{n+1/2},\mathbf{x}) + V^{\mathrm{ext}}(t_{n+1/2},\mathbf{x})) + V(t_{n+1},\mathbf{x}) + V^{\mathrm{ext}}(t_{n+1},\mathbf{x})\right], \\ \mathbf{A}^{n+1/2}(\mathbf{x}) &= \left(A_1^{n+1/2}(\mathbf{x}), A_2^{n+1/2}(\mathbf{x}), A_3^{n+1/2}(\mathbf{x})\right)^{\mathrm{T}}, \quad \mathbf{x}\in\Omega, \\ A_k^{n+1/2}(\mathbf{x}) &= \frac{1}{6}\left[A_k(t_n,\mathbf{x}) + A_k^{\mathrm{ext}}(t_n,\mathbf{x}) + 4(A_k(t_{n+1/2},\mathbf{x}) \right. \\ &\quad \left. + A_k^{\mathrm{ext}}(t_{n+1/2},\mathbf{x})) + A_k(t_{n+1},\mathbf{x}) + A_k^{\mathrm{ext}}(t_{n+1},\mathbf{x})\right], \quad k = 1,2,3. \end{aligned}$$

Since $G^{n+1/2}(\mathbf{x})$ is a U-matrix, it is diagonalizable. The characteristic polynomial of $G^{n+1/2}(\mathbf{x})$ is

$$\begin{aligned} \det\left(\lambda\mathbb{I}_4 - G^{n+1/2}(\mathbf{x})\right) &= \begin{vmatrix} \lambda - V^{n+1/2}(\mathbf{x}) & 0 & A_3^{n+1/2}(\mathbf{x}) & A_-^{n+1/2}(\mathbf{x}) \\ 0 & \lambda - V^{n+1/2}(\mathbf{x}) & A_+^{n+1/2}(\mathbf{x}) & -A_3^{n+1/2}(\mathbf{x}) \\ A_3^{n+1/2}(\mathbf{x}) & A_-^{n+1/2}(\mathbf{x}) & \lambda - V^{n+1/2}(\mathbf{x}) & 0 \\ A_+^{n+1/2}(\mathbf{x}) & -A_3^{n+1/2}(\mathbf{x}) & 0 & \lambda - V^{n+1/2}(\mathbf{x}) \end{vmatrix} \\ &= \left[\left(\lambda - V^{n+1/2}(\mathbf{x})\right)^2 - |\mathbf{A}^{n+1/2}(\mathbf{x})|^2\right]^2 = 0. \end{aligned} \tag{A.2}$$

Thus the eigenvalues of $G^{n+1/2}(\mathbf{x})$ are

$$\lambda_+^{n+1/2}(\mathbf{x}), \quad \lambda_+^{n+1/2}(\mathbf{x}), \quad \lambda_-^{n+1/2}(\mathbf{x}), \quad \lambda_-^{n+1/2}(\mathbf{x})$$

with

$$\lambda_{\pm}^{n+1/2}(\mathbf{x}) = V^{n+1/2}(\mathbf{x}) \pm |\mathbf{A}^{n+1/2}(\mathbf{x})| = V^{n+1/2}(\mathbf{x}) \pm \sqrt{\sum_{j=1}^{3} |A_j^{n+1/2}(\mathbf{x})|^2}$$

and the corresponding eigenvectors are

$$\mathbf{v}_1^{n+1/2}(\mathbf{x}) = \begin{pmatrix} A_-^{n+1/2}(\mathbf{x}) \\ -A_3^{n+1/2}(\mathbf{x}) \\ 0 \\ |\mathbf{A}^{n+1/2}(\mathbf{x})| \end{pmatrix}, \quad \mathbf{v}_2^{n+1/2}(\mathbf{x}) = \begin{pmatrix} A_3^{n+1/2}(\mathbf{x}) \\ A_+^{n+1/2}(\mathbf{x}) \\ |\mathbf{A}^{n+1/2}(\mathbf{x})| \\ 0 \end{pmatrix},$$

$$\mathbf{v}_3^{n+1/2}(\mathbf{x}) = \begin{pmatrix} 0 \\ -|\mathbf{A}^{n+1/2}(\mathbf{x})| \\ A_-^{n+1/2}(\mathbf{x}) \\ -A_3^{n+1/2}(\mathbf{x}) \end{pmatrix}, \quad \mathbf{v}_4^{n+1/2}(\mathbf{x}) = \begin{pmatrix} -|\mathbf{A}^{n+1/2}(\mathbf{x})| \\ 0 \\ A_3^{n+1/2}(\mathbf{x}) \\ A_+^{n+1/2}(\mathbf{x}) \end{pmatrix},$$

Let

$$D^{n+1/2}(\mathbf{x}) = \mathrm{diag}\Big(\lambda_+^{n+1/2}(\mathbf{x}), \lambda_+^{n+1/2}(\mathbf{x}), \lambda_-^{n+1/2}(\mathbf{x}), \lambda_-^{n+1/2}(\mathbf{x})\Big),$$

$$P^{n+1/2}(\mathbf{x}) = \frac{1}{\sqrt{2}|\mathbf{A}^{n+1/2}(\mathbf{x})|}\Big(\mathbf{v}_1^{n+1/2}(\mathbf{x}) \quad \mathbf{v}_2^{n+1/2}(\mathbf{x}) \quad \mathbf{v}_3^{n+1/2}(\mathbf{x}) \quad \mathbf{v}_4^{n+1/2}(\mathbf{x})\Big).$$

Thus $D^{n+1/2}(\mathbf{x})$ is a diagonal matrix, $P^{n+1/2}(\mathbf{x})$ is a complex orthogonormal matrix, and they diagonalize the matrix $G^{n+1/2}(\mathbf{x})$, i.e.

$$G^{n+1/2}(\mathbf{x}) = P^{n+1/2}(\mathbf{x}) D^{n+1/2}(\mathbf{x}) (\bar{P}^{n+1/2}(\mathbf{x}))^{\mathrm{T}}, \quad \mathbf{x} \in \Omega. \tag{A.3}$$

In order to compute $G^{n+1/2}(\mathbf{x}_{p,q,r})$ ($(p,q,r) \in \mathscr{M}$) used in (A.1), we need $V(t_n, \mathbf{x}_{p,q,r}) = V_{p,q,r}^n$, $V(t_{n+1}, \mathbf{x}_{p,q,r}) = V_{p,q,r}^{n+1}$, $\mathbf{A}(t_n, \mathbf{x}_{p,q,r}) = \mathbf{A}_{p,q,r}^n$, $\mathbf{A}(t_{n+1}, \mathbf{x}_{p,q,r}) = \mathbf{A}_{p,q,r}^{n+1}$, $V(t_{n+1/2}, \mathbf{x}_{p,q,r})$ and $\mathbf{A}(t_{n+1/2}, \mathbf{x}_{p,q,r})$. The first four terms are given in (3.27) and (3.28). The last two terms can be computed as following:

$$V(t_{n+1/2}, \mathbf{x}_{p,q,r}) = \sum_{(j,k,l)\in\mathscr{M}} \widetilde{V}_{j,k,l}^n(t_{n+1/2})\ \mathrm{e}^{\mathrm{i}\mu_{j,k,l}\cdot(\mathbf{x}_{p,q,r}-\mathbf{a})},$$

$$\mathbf{A}(t_{n+1/2}, \mathbf{x}_{p,q,r}) = \sum_{(j,k,l)\in\mathscr{M}} \widetilde{\mathbf{A}}_{j,k,l}^n(t_{n+1/2})\ \mathrm{e}^{\mathrm{i}\mu_{j,k,l}\cdot(\mathbf{x}_{p,q,r}-\mathbf{a})},$$

where for $n = 0$:

$$\widetilde{V}_{j,k,l}^0(t_{1/2}) = \begin{cases} (\widetilde{V^{(0)}})_{j,k,l} + \frac{\Delta t}{2}(\widetilde{V^{(1)}})_{j,k,l} + (\widetilde{|\Psi^{(0)}|^2})_{j,k,l}(\Delta t)^2/8\varepsilon^2, & j=k=l=0, \\ \left[(\widetilde{V^{(0)}})_{j,k,l} - (\widetilde{|\Psi^{(0)}|^2})_{j,k,l}/|\mu_{j,k,l}|^2\right]\cos(\Delta t|\mu_{j,k,l}|/2\varepsilon) & \\ \quad + (\widetilde{V^{(1)}})_{j,k,l}\sin(\Delta t|\mu_{j,k,l}|/2\varepsilon)\frac{\varepsilon}{|\mu_{j,k,l}|} & \\ \quad + (\widetilde{|\Psi^{(0)}|^2})_{j,k,l}/|\mu_{j,k,l}|^2 & \text{otherwise.} \end{cases}$$

$$\widetilde{\mathbf{A}}^{0}_{j,k,l}(t_{1/2}) = \begin{cases} (\widetilde{\mathbf{A}^{(0)}})_{j,k,l} + \frac{\Delta t}{2}(\widetilde{\mathbf{A}^{(1)}})_{j,k,l} + (\widetilde{\mathbf{J}^{(0)}})_{j,k,l}(\Delta t)^2/8\varepsilon^2, & j=k=l=0, \\ \left[(\widetilde{\mathbf{A}^{(0)}})_{j,k,l} - (\widetilde{\mathbf{J}^{(0)}})_{j,k,l}/|\mu_{j,k,l}|^2\right]\cos(\Delta t|\mu_{j,k,l}|/2\varepsilon) \\ \quad +(\widetilde{\mathbf{A}^{(1)}})_{j,k,l}\sin(\Delta|\mu_{j,k,l}|/2\varepsilon)\frac{\varepsilon}{|\mu_{j,k,l}|} \\ \quad +(\widetilde{\mathbf{J}^{(0)}})_{j,k,l}/|\mu_{j,k,l}|^2 & \text{otherwise.} \end{cases}$$

and for $n > 0$:

$$\widetilde{V}^{n}_{j,k,l}(t_{n+1/2}) = \begin{cases} \frac{3}{2}\widetilde{V}^{n}_{j,k,l}(t_n) - \frac{1}{2}\widetilde{V}^{n-1}_{j,k,l}(t_{n-1}) + 3(\widetilde{|\Psi^n|^2})_{j,k,l}(\Delta t)^2/8\varepsilon^2, & j=k=l=0, \\ \left[\widetilde{V}^{n}_{j,k,l} - (\widetilde{|\Psi^n|^2})_{j,k,l}/|\mu_{j,k,l}|^2\right]\cos(\Delta t|\mu_{j,k,l}|/2\varepsilon) \\ \quad +\Big[(1-\cos(|\mu_{j,k,l}|\Delta t/\varepsilon))(\widetilde{|\Psi^n|^2})_{j,k,l}/|\mu_{j,k,l}|^2 \\ \quad -\widetilde{V}^{n-1}_{j,k,l}(t_{n-1}) + \widetilde{V}^{n}_{j,k,l}(t_n)\cos(|\mu_{j,k,l}|\Delta t/\varepsilon)\Big] \\ \quad \times\frac{1}{2\cos(|\mu_{j,k,l}|\Delta t/2\varepsilon)} + (\widetilde{|\Psi^n|^2})_{j,k,l}/|\mu_{j,k,l}|^2 & \text{otherwise.} \end{cases}$$

$$\widetilde{\mathbf{A}}^{n}_{j,k,l}(t_{n+1/2}) = \begin{cases} \frac{3}{2}\widetilde{\mathbf{A}}^{n}_{j,k,l}(t_n) - \frac{1}{2}\widetilde{\mathbf{A}}^{n-1}_{j,k,l}(t_{n-1}) + 3(\widetilde{\mathbf{J}^{(n)}})_{j,k,l}(\Delta t)^2/8\varepsilon^2, & j=k=l=0, \\ \left[\widetilde{\mathbf{A}}^{n}_{j,k,l} - (\widetilde{\mathbf{J}^{(n)}})_{j,k,l}/|\mu_{j,k,l}|^2\right]\cos(\Delta t|\mu_{j,k,l}|/2\varepsilon) \\ \quad +\Big[(1-\cos(|\mu_{j,k,l}|\Delta t/\varepsilon))(\widetilde{\mathbf{J}^{(n)}})_{j,k,l}/|\mu_{j,k,l}|^2 \\ \quad -\widetilde{\mathbf{A}}^{n-1}_{j,k,l}(t_{n-1}) + \widetilde{\mathbf{A}}^{n}_{j,k,l}(t_n)\cos(|\mu_{j,k,l}|\Delta t/\varepsilon)\Big] \\ \quad \times\frac{1}{2\cos(|\mu_{j,k,l}|\Delta t/2\varepsilon)} + (\widetilde{\mathbf{J}^{(n)}})_{j,k,l}/|\mu_{j,k,l}|^2 & \text{otherwise.} \end{cases}$$

The discretized current density $\mathbf{J}^{(n)}$ is computed as

$$\mathbf{J}^{(n)}_{p,q,r} = \left((j^{(n)}_1)_{p,q,r},\quad (j^{(n)}_2)_{p,q,r},\quad (j^{(n)}_3)_{p,q,r}\right)^{\mathrm{T}},$$
$$(j^{(n)}_k)_{p,q,r} = \langle \Psi^n_{p,q,r}, \alpha^k \Psi^n_{p,q,r}\rangle,\quad k=1,2,3,\ \ n\geqslant 0\ (p,q,r)\in\mathcal{N}.$$

Appendix B. Diagnolize the matrix $M_{j,k,l}$ in (3.24)

From (3.24), notice (1.7), we have

$$M_{j,k,l} = \mu^{(1)}_j\alpha^1 + \mu^{(2)}_k\alpha^2 + \mu^{(3)}_l\alpha^3 + \varepsilon^{-1}\delta^{-1} = \begin{pmatrix} \varepsilon^{-1}\delta^{-1} & 0 & \mu^{(3)}_l & \mu^{(1)}_j - \mathrm{i}\mu^{(2)}_k \\ 0 & \varepsilon^{-1}\delta^{-1} & \mu^{(1)}_j + \mathrm{i}\mu^{(2)}_k & -\mu^{(3)}_l \\ \mu^{(3)}_l & \mu^{(1)}_j - \mathrm{i}\mu^{(2)}_k & -\varepsilon^{-1}\delta^{-1} & 0 \\ \mu^{(1)}_j + \mathrm{i}\mu^{(2)}_k & -\mu^{(3)}_l & 0 & -\varepsilon^{-1}\delta^{-1} \end{pmatrix}.$$

The characteristic polynomial of $M_{j,k,l}$ is

$$\det\left(\lambda\mathbb{I}_4 - M_{j,k,l}\right) = \begin{vmatrix} \lambda - \varepsilon^{-1}\delta^{-1} & 0 & -\mu_l^{(3)} & -\mu_j^{(1)} + \mathrm{i}\mu_k^{(2)} \\ 0 & \lambda - \varepsilon^{-1}\delta^{-1} & -\mu_j^{(1)} - \mathrm{i}\mu_k^{(2)} & \mu l^{(3)} \\ -\mu_l^{(3)} & -\mu_j^{(1)} + \mathrm{i}\mu_k^{(2)} & \lambda + \varepsilon^{-1}\delta^{-1} & 0 \\ -\mu_j^{(1)} - \mathrm{i}\mu_k^{(2)} & \mu_l^{(3)} & 0 & \lambda + \varepsilon^{-1}\delta^{-1} \end{vmatrix}$$
$$= \left(\lambda^2 - \varepsilon^{-2}\delta^{-2} - |\mu_{j,k,l}|^2\right)^2 = 0. \tag{B.1}$$

Thus the eigenvalues of $M_{j,k,l}$ are

$$\lambda_{j,k,l}, \quad \lambda_{j,k,l}, \quad -\lambda_{j,k,l}, \quad -\lambda_{j,k,l} \quad \text{with } \lambda_{j,k,l} = \sqrt{\varepsilon^{-2}\delta^{-2} + |\mu_{j,k,l}|^2}$$

and the corresponding eigenvectors are

$$\mathbf{v}_{j,k,l}^1 = \begin{pmatrix} \lambda_{j,k,l} + \varepsilon^{-1}\delta^{-1} \\ 0 \\ \mu_l^{(3)} \\ \mu_j^{(1)} + \mathrm{i}\mu_k^{(2)} \end{pmatrix}, \quad \mathbf{v}_{j,k,l}^2 = \begin{pmatrix} 0 \\ \lambda_{j,k,l} + \varepsilon^{-1}\delta^{-1} \\ \mu_j^{(1)} - \mathrm{i}\mu_k^{(2)} \\ -\mu_l^{(3)} \end{pmatrix},$$
$$\mathbf{v}_{j,k,l}^3 = \begin{pmatrix} -\mu_l^{(3)} \\ -\mu_j^{(1)} - \mathrm{i}\mu_k^{(2)} \\ \lambda_{j,k,l} + \varepsilon^{-1}\delta^{-1} \\ 0 \end{pmatrix}, \quad \mathbf{v}_{j,k,l}^4 = \begin{pmatrix} -\mu_j^{(1)} + \mathrm{i}\mu_k^{(2)} \\ \mu_l^{(3)} \\ 0 \\ \lambda_{j,k,l} + \varepsilon^{-1}\delta^{-1} \end{pmatrix}.$$

Let

$$D_{j,k,l} = \mathrm{diag}\left(\lambda_{j,k,l}, \lambda_{j,k,l}, -\lambda_{j,k,l}, -\lambda_{j,k,l}\right),$$
$$P_{j,k,l} = \frac{1}{\sqrt{2(\lambda_{j,k,l}^2 + \varepsilon^{-1}\delta^{-1}\lambda_{j,k,l})}}\left(\mathbf{v}_{j,k,l}^1 \quad \mathbf{v}_{j,k,l}^2 \quad \mathbf{v}_{j,k,l}^3 \quad \mathbf{v}_{j,k,l}^4\right).$$

Thus $D_{j,k,l}$ is a diagonal matrix, $P_{j,k,l}$ is a complex orthogonormal matrix, and they diagonalize the matrix $M_{j,k,l}$, i.e.

$$M_{j,k,l} = P_{j,k,l} D_{j,k,l} (\bar{P}_{j,k,l})^{\mathrm{T}} \quad (j,k,l) \in \mathscr{M}. \tag{B.2}$$

Appendix C. Computation of $\widetilde{V}_{j,k,l}^n(t_{n+1})$ and $\widetilde{V}_{j,k,l}^n(t_{n+1})$ in (3.27) and (3.28)

For $n = 0$:

$$\widetilde{V}_{j,k,l}^0(t_1) = \begin{cases} (\widetilde{V^{(0)}})_{j,k,l} + \Delta t(\widetilde{V^{(1)}})_{j,k,l} + (\widetilde{|\Psi^{(0)}|^2})_{j,k,l}(\Delta t)^2/2\varepsilon^2, & j = k = l = 0, \\ \left[(\widetilde{V^{(0)}})_{j,k,l} - (\widetilde{|\Psi^{(0)}|^2})_{j,k,l}|\mu_{j,k,l}|^2\right]\cos(\Delta t|\mu_{j,k,l}|/\varepsilon) & \\ \quad + (\widetilde{V^{(1)}})_{j,k,l}\sin(\Delta t|\mu_{j,k,l}|/\varepsilon)\frac{\varepsilon}{|\mu_{j,k,l}|} & \\ \quad + (\widetilde{|\Psi^{(0)}|^2})_{j,k,l}/|\mu_{j,k,l}|^2 & \text{otherwise.} \end{cases} \tag{C.1}$$

$$\widetilde{\mathbf{A}}^0_{j,k,l}(t_1) = \begin{cases} (\widetilde{\mathbf{A}^{(0)}})_{j,k,l} + \Delta t(\widetilde{\mathbf{A}^{(1)}})_{j,k,l} + (\widetilde{\mathbf{J}^{(0)}})_{j,k,l}(\Delta t)^2/2\varepsilon^2, & j=k=l=0, \\ \left[(\widetilde{\mathbf{A}^{(0)}})_{j,k,l} - (\widetilde{\mathbf{J}^{(0)}})_{j,k,l}/|\mu_{j,k,l}|^2\right]\cos(\Delta t|\mu_{j,k,l}|/\varepsilon) & \\ \quad +(\widetilde{\mathbf{A}^{(1)}})_{j,k,l}\sin(\Delta t|\mu_{j,k,l}|/\varepsilon)\frac{\varepsilon}{|\mu_{j,k,l}|} & \\ \quad +(\widetilde{\mathbf{J}^{(0)}})_{j,k,l}/|\mu_{j,k,l}|^2 & \text{otherwise.} \end{cases} \tag{C.2}$$

and for $n > 0$:

$$\widetilde{V}^n_{j,k,l}(t_{n+1}) = \begin{cases} 2\widetilde{V}^n_{j,k,l}(t_n) - \widetilde{V}^{n-1}_{j,k,l}(t_{n-1}) + (\widetilde{|\Psi^n|^2})_{j,k,l}(\Delta t)^2/\varepsilon^2, & j=k=l=0, \\ 2\left[\widetilde{V}^n_{j,k,l} - (\widetilde{|\Psi^n|^2})_{j,k,l}/|\mu_{j,k,l}|^2\right]\cos(\Delta t|\mu_{j,k,l}|/\varepsilon) & \\ \quad -\widetilde{V}^{n-1}_{j,k,l}(t_{n-1}) + 2(\widetilde{|\Psi^n|^2})_{j,k,l}/|\mu_{j,k,l}|^2 & \text{otherwise.} \end{cases} \tag{C.3}$$

$$\widetilde{\mathbf{A}}^n_{j,k,l}(t_{n+1}) = \begin{cases} 2\widetilde{\mathbf{A}}^n_{j,k,l}(t_n) - \widetilde{\mathbf{A}}^{n-1}_{j,k,l}(t_{n-1}) + (\widetilde{\mathbf{J}^{(n)}})_{j,k,l}(\Delta t)^2/\varepsilon^2, & j=k=l=0, \\ 2\left[\widetilde{\mathbf{A}}^n_{j,k,l} - (\widetilde{\mathbf{J}^{(n)}})_{j,k,l}/|\mu_{j,k,l}|^2\right]\cos(\Delta t|\mu_{j,k,l}|/\varepsilon) & \\ \quad -\widetilde{\mathbf{A}}^{n-1}_{j,k,l}(t_{n-1}) + 2(\widetilde{\mathbf{J}^{(n)}})_{j,k,l}/|\mu_{j,k,l}|^2 & \text{otherwise.} \end{cases} \tag{C.4}$$

Appendix D. Proof of Theorem 3.1

Proof. From (3.29), notice (3.30), (3.20) and (3.25), Parseval's equality, we have

$$\begin{aligned} \frac{1}{h_1h_2h_3}\|\Psi^{n+1}\|_{l^2}^2 &= \sum_{(p,q,r)\in\mathcal{Q}}\left|\Psi^{n+1}_{p,q,r}\right|^2 \\ &= \sum_{(p,q,r)\in\mathcal{Q}}\left|\sum_{(j,k,l)\in\mathcal{M}} P_{j,k,l}\exp\left[-\frac{\mathrm{i}\Delta t}{2\varepsilon}D_{j,k,l}\right](\bar{P}_{j,k,l})^{\mathrm{T}}(\widetilde{\Psi^{**}})_{j,k,l}\mathrm{e}^{\mathrm{i}\mu_{j,k,l}\cdot(\mathbf{x}_{p,q,r}-\mathbf{a})}\right|^2 \\ &= M_1M_2M_3\sum_{(j,k,l)\in\mathcal{M}}\left|P_{j,k,l}\exp\left[-\frac{\mathrm{i}\Delta t}{2\varepsilon}D_{j,k,l}\right](\bar{P}_{j,k,l})^{\mathrm{T}}(\widetilde{\Psi^{**}})_{j,k,l}\right|^2 \\ &= M_1M_2M_3\sum_{(j,k,l)\in\mathcal{M}}\left|(\widetilde{\Psi^{**}})_{j,k,l}\right|^2 \\ &= \frac{1}{M_1M_2M_3}\sum_{(j,k,l)\in\mathcal{M}}\left|\sum_{(p,q,r)\in\mathcal{Q}}\Psi^{**}_{p,q,r}\mathrm{e}^{\mathrm{i}\mu_{j,k,l}\cdot(\mathbf{x}_{p,q,r}-\mathbf{a})}\right|^2 = \sum_{(p,q,r)\in\mathcal{Q}}|\Psi^{**}|^2 \\ &= \sum_{(p,q,r)\in\mathcal{Q}}\left|P^{n+1/2}(\mathbf{x}_{p,q,r})\exp\left[-i\frac{\Delta t}{\delta}D^{n+1/2}(\mathbf{x}_{p,q,r})\right](\bar{P}^{n+1/2}(\mathbf{x}_{p,q,r}))^{\mathrm{T}}\Psi^*_{p,q,r}\right|^2 \\ &= \sum_{(p,q,r)\in\mathcal{Q}}\left|\Psi^*_{p,q,r}\right|^2 = \sum_{(p,q,r)\in\mathcal{Q}}\left|\Psi^n_{p,q,r}\right|^2 = \frac{1}{h_1h_2h_3}\|\Psi^n\|_{l^2}^2, \quad n\geqslant 0. \end{aligned} \tag{D.1}$$

Thus the equality (3.34) is obtained by induction.

From (3.27), notice (C.1), (C.3), (3.30), we have

$$\begin{aligned}\widetilde{V}^{n}_{0,0,0}(t_{n+1}) &= 2\widetilde{V}^{n}_{0,0,0}(t_n) - \widetilde{V}^{n-1}_{0,0,0}(t_{n-1}) + \widetilde{(|\Psi^n|^2)}_{0,0,0}(\Delta t)^2/\varepsilon^2 \\ &= 2\widetilde{V}^{n}_{0,0,0}(t_n) - \widetilde{V}^{n-1}_{0,0,0}(t_{n-1}) + \frac{(\Delta t)^2}{M_1M_2M_3\varepsilon^2}\sum_{(p,q,r)\in\mathcal{L}}|\Psi^{(0)}_{p,q,r}|^2 \\ &= 2\widetilde{V}^{n-1}_{0,0,0}(t_n) - \widetilde{V}^{n-1}_{0,0,0}(t_{n-1}) + \frac{(\Delta t)^2}{M_1M_2M_3\varepsilon^2}\sum_{(p,q,r)\in\mathcal{L}}|\Psi^{(0)}_{p,q,r}|^2 \\ &= 3\widetilde{V}^{n-2}_{0,0,0}(t_{n-1}) - 2\widetilde{V}^{n-2}_{0,0,0}(t_{n-2}) + \frac{(1+2)(\Delta t)^2}{M_1M_2M_3\varepsilon^2}\sum_{(p,q,r)\in\mathcal{L}}|\Psi^{(0)}_{p,q,r}|^2. \end{aligned} \tag{D.2}$$

By induction, we get

$$\begin{aligned}\widetilde{V}^{n}_{0,0,0}(t_{n+1}) &= (n+1)\widetilde{V}^{0}_{0,0,0}(t_1) - n\widetilde{V}^{0}_{0,0,0}(t_0) + \frac{n(n+1)(\Delta t)^2}{2M_1M_2M_3\varepsilon^2}\sum_{(p,q,r)\in\mathcal{L}}|\Psi^{(0)}_{p,q,r}|^2 \\ &= \widetilde{V}^{(0)}_{0,0,0}(t_0) + t_{n+1}\widetilde{V}^{(1)}_{0,0,0}(t_0) + \frac{t^2_{n+1}}{2M_1M_2M_3\varepsilon^2}\sum_{(p,q,r)\in\mathcal{L}}|\Psi^{(0)}_{p,q,r}|^2, \quad n\geqslant 0. \end{aligned} \tag{D.3}$$

From (3.27), notice (D.3), (3.30) and (3.32), we get

$$\begin{aligned}\frac{1}{h_1h_2h_3}\mathrm{DMean}(V^{n+1}) &= \sum_{(p,q,r)\in\mathcal{L}}V^{n+1}_{p,q,r} = \sum_{(p,q,r)\in\mathcal{L}}\sum_{(j,k,l)\in\mathcal{M}}\widetilde{V}^{n}_{j,k,l}(t_{n+1})\mathrm{e}^{\mathrm{i}\mu_{j,k,l}\cdot(\mathbf{x}_{p,q,r}-\mathbf{a})} \\ &= \sum_{(j,k,l)\in\mathcal{M}}\widetilde{V}^{n}_{j,k,l}(t_{n+1})\sum_{(p,q,r)\in\mathcal{L}}\mathrm{e}^{\mathrm{i}\mu_{j,k,l}\cdot(\mathbf{x}_{p,q,r}-\mathbf{a})} = M_1M_2M_3\widetilde{V}^{n}_{0,0,0}(t_{n+1}) \\ &= M_1M_2M_3\left[\widetilde{V}^{0}_{0,0,0}(t_0) + t_{n+1}\widetilde{V}^{(1)}_{0,0,0}(t_0)\right] + \frac{t^2_{n+1}}{2\varepsilon^2}\sum_{(p,q,r)\in\mathcal{L}}|\Psi^{(0)}_{p,q,r}|^2 \\ &= \sum_{(p,q,r)\in\mathcal{L}}V^{(0)}_{p,q,r} + t_{n+1}\sum_{(p,q,r)\in\mathcal{L}}V^{(1)}_{p,q,r} + \frac{t^2_{n+1}}{2\varepsilon^2}\sum_{(p,q,r)\in\mathcal{L}}|\Psi^{(0)}_{p,q,r}|^2, \quad n\geqslant 0. \end{aligned} \tag{D.4}$$

Thus the desired equality (3.35) is a combination of (3.32) and (D.4). □

References

[1] S. Abenda, Solitary waves for Maxwell–Dirac and Coulomb–Dirac models, Ann. Inst. H. Poincare Phys. Theor. 68 (1998) 229–244.
[2] W. Bao, D. Jaksch, An explicit unconditionally stable numerical methods for solving damped nonlinear Schrödinger equations with a focusing nonlinearity, SIAM J. Numer. Anal. 41 (2003) 1406–1426.
[3] W. Bao, D. Jaksch, P.A. Markowich, Numerical solution of the Gross–Pitaevskii equation for Bose–Einstein condensation, J. Comput. Phys. 187 (2003) 318–342.
[4] W. Bao, S. Jin, P.A. Markowich, On time-splitting spectral approximations for the Schrödinger equation in the semiclassical regime, J. Comput. Phys. 175 (2002) 487–524.
[5] W. Bao, S. Jin, P.A. Markowich, Numerical study of time-splitting spectral discretizations of nonlinear Schrödinger equations in the semi-clasical regimes, SIAM J. Sci. Comput. 25 (2003) 27–64.
[6] W. Bao, F. Sun, Efficient and stable numerical methods for the generalized and vector Zakharov system, SIAM J. Sci. Comput. (in press).

[7] W. Bao, F. Sun, G.W. Wei, Numerical methods for the generalized Zakharov system, J. Comput. Phys. 190 (2003) 201–228.
[8] P. Bechouche, N.J. Mauser, F. Poupaud, (Semi)-nonrelativistic limits of the Dirac equation with external time-dependent electromagnetic field, Commun. Math. Phys. 197 (1998) 405–425.
[9] J. Bolte, S. Keppeler, A semiclassical approach to the Dirac equation, Ann. Phys. 274 (1999) 125–162.
[10] H.S. Booth, G. Legg, P.D. Jarvis, Algebraic solution for the vector potential in the Dirac equation, J. Phys. A 34 (2001) 5667–5677.
[11] N. Bournaveas, Local existence for the Maxwell–Dirac equations in three space dimensions, Commun. Partial Differential Equations 21 (1996) 693–720.
[12] J.M. Chadam, Global solutions of the Cauchy problem for the (classical) coupled Maxwell–Dirac equations in one space dimension, J. Funct. Anal. 13 (1973) 173–184.
[13] A. Das, General solutions of Maxwell–Dirac equations in 1 + 1-dimensional space–time and a spatially confined solution, J. Math. Phys 34 (1993) 3985–3986.
[14] A. Das, An ongoing big bang model in the special relativistic Maxwell–Dirac equations, J. Math. Phys. 37 (1996) 2253–2259.
[15] A. Das, D. Kay, A class of exact plane wave solutions of the Maxwell–Dirac equations, J. Math. Phys. 30 (1989) 2280–2284.
[16] P.A.M. Dirac, Principles of Quantum Mechanics, Oxford University Press, London, 1958.
[17] M. Esteban, E. Sere, An overview on linear and nonlinear Dirac equations, Discrete Contin. Dyn. Syst. 8 (2002) 381–397.
[18] C. Fermanian-Kammerer, Semi-classical analysis of a Dirac equation without adiabatic decoupling, Monatsh. Math. (to appear).
[19] M. Flato, J.C.H. Simon, E. Taflin, Asymptotic completeness, global existence and the infrared problem for the Maxwell–Dirac equations, Mem. Am. Math. Soc. 127 (1997) 311.
[20] V. Georgiev, Small amplitude solutions of the Maxwell–Dirac equations, Indiana Univ. Math. J. 40 (1991) 845–883.
[21] L. Gross, The Cauchy problem for coupled Maxwell and Dirac equations, Commun. Pure Appl. Math. 19 (1966) 1–15.
[22] W. Hunziker, On the nonrelativistic limit of the Dirac theory, Commun. Math. Phys. 40 (1975) 215–222.
[23] A.G. Lisi, A solitary wave solution of the Maxwell–Dirac equations, J. Phys. A 28 (1995) 5385–5392.
[24] N. Masmoudi, N.J. Mauser, The selfconsistent Pauli equation, Monatsh. Math. 132 (2001) 19–24.
[25] B. Najman, The nonrelativstic limit of the nonlinear Dirac equation, Ann. Inst. Henri Poincare Non Lineaire 9 (1992) 3–12.
[26] C. Sparber, P. Markowich, Semiclassical asymptotics for the Maxwell–Dirac system, J. Math. Phys. 44 (2003) 4555–4572.
[27] H. Spohn, Semiclassical limit of the Dirac equation and spin precession, Ann. Phys. 282 (2000) 420–431.
[28] B. Thaller, The Dirac Equation, Springer, New York, 1992.